Amyloid Probe

-Insights into Its Binding Sites and Selectivity-

Literature Seminar #2

2021/10/14

Wataru Atsumi (B5)

Table of contents

Amyloids and human diseases

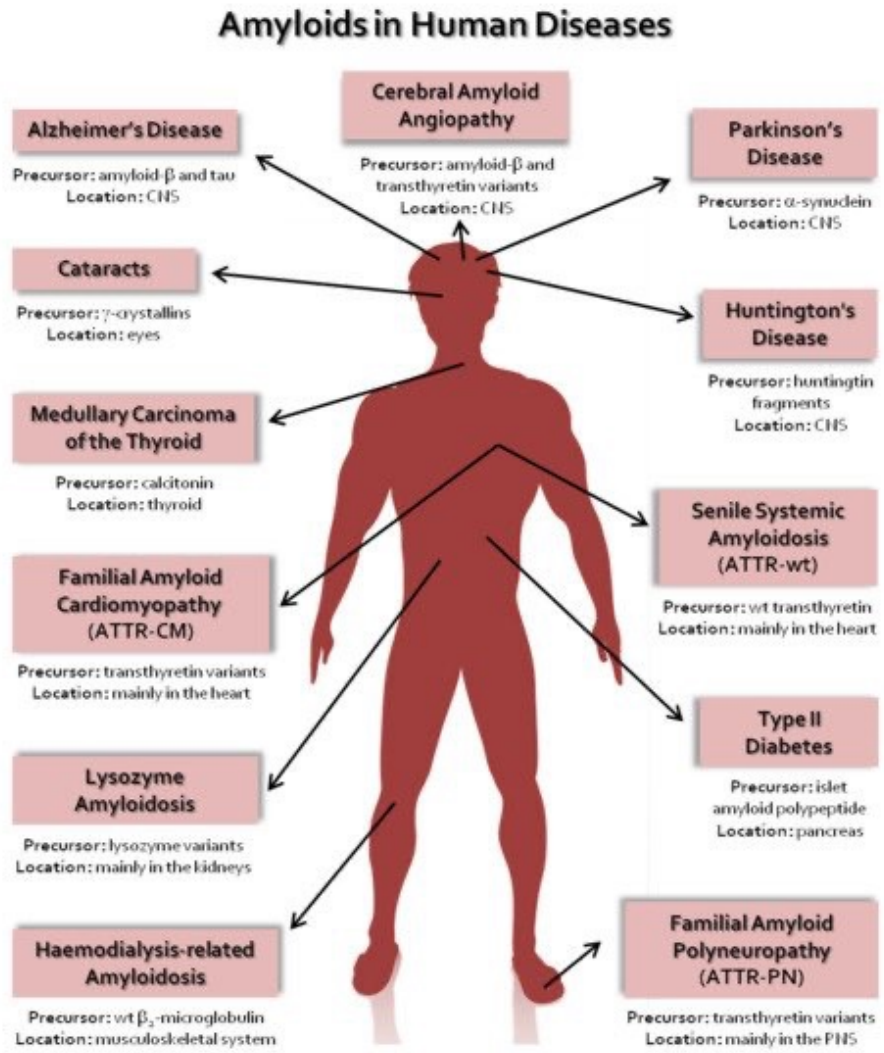

The aggregation of peptides into **amyloid fibrils** is the hallmark of misfolding diseases known as **amyloidosis**.

e.g.

- **Alzheimer's disease**
- **Perkinson's disease**
- **Huntington's disease**

Zaida L. Almeida and Rui M. M. Brito, *Molecules,* **2020**, *25*(5), 1195.

The process of amyloid formation

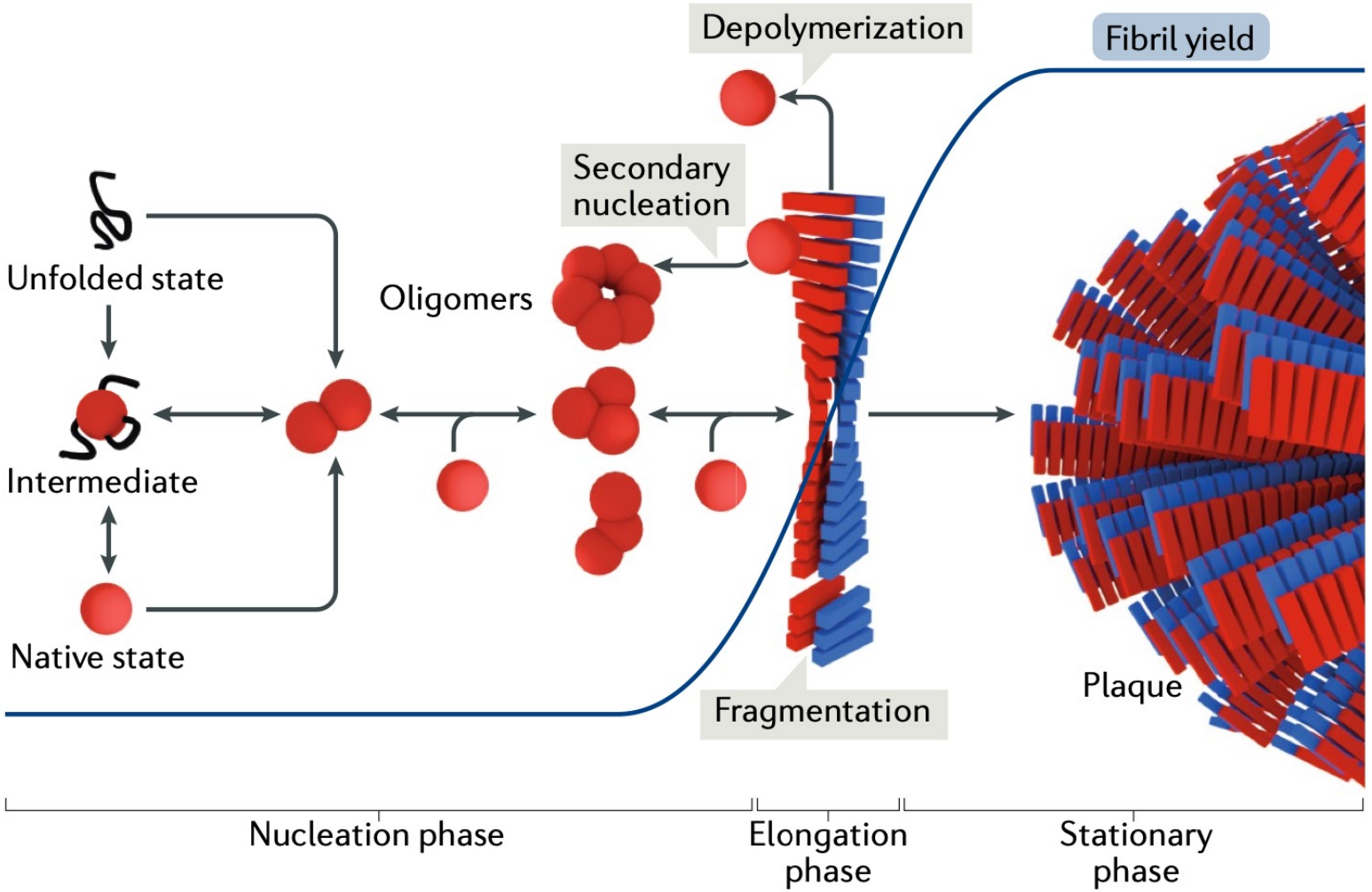

Iadanza, M.G., Jackson, M.P., Hewitt, E.W. *et al. Nat Rev. Mol. Cell Biol.* **2018**, 19, 755–773.

Cytotoxicity of amyloids

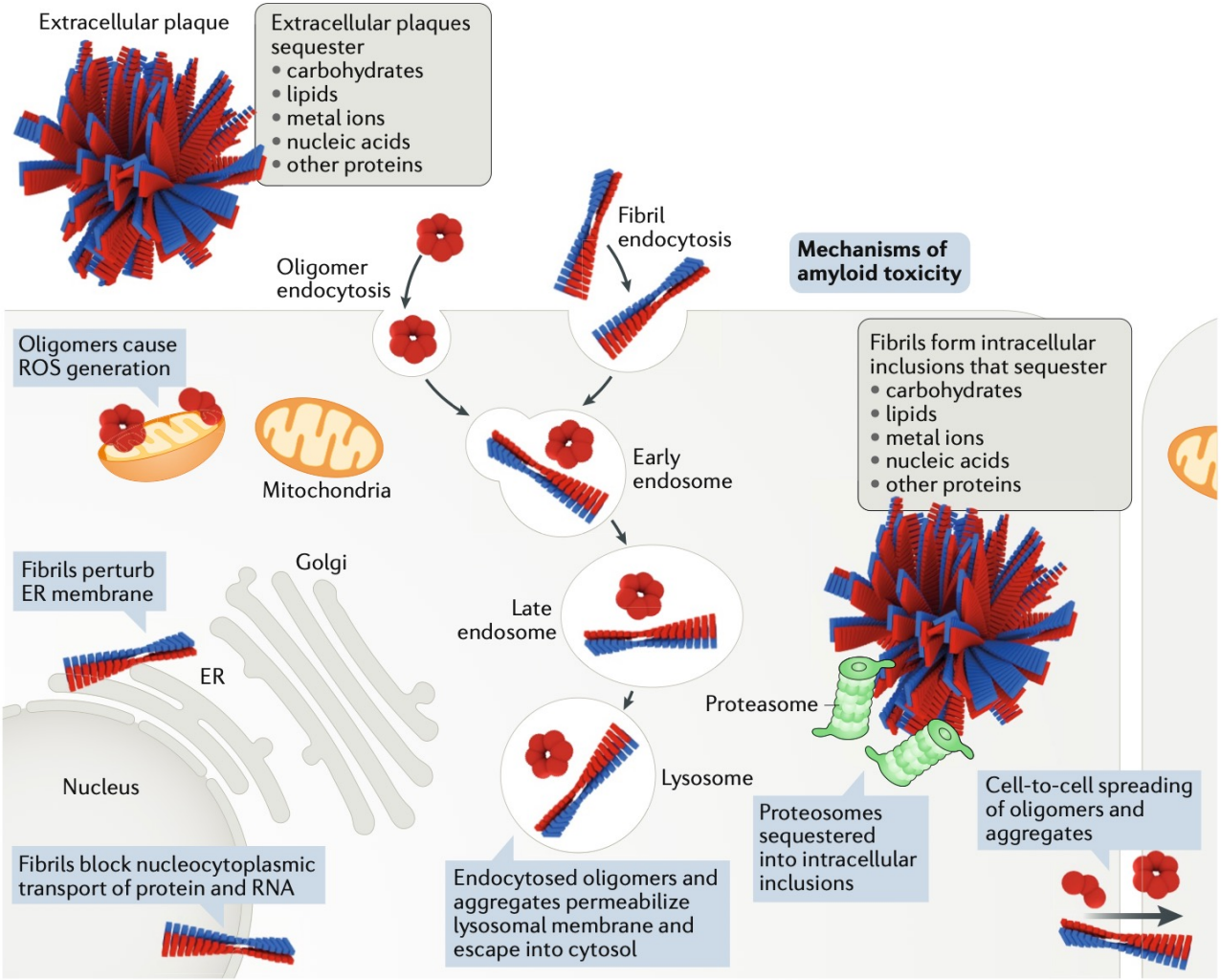

Not only fibrils but oligomers represent cytotoxicity.

Iadanza, M.G., Jackson, M.P., Hewitt, E.W. *et al. Nat Rev. Mol. Cell Biol.* **2018**, 19, 755–773.

Fluorescent probe for amyloid

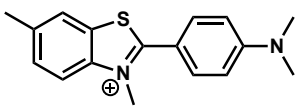

Thioflavin T (ThT)

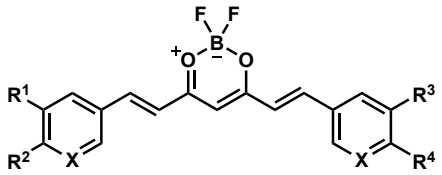

CRANAD

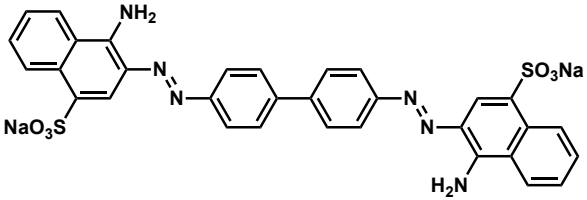

Congo Red (CR)

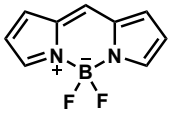

BODIPY

The strengths of fluorescent probe

- ✓ **Real-time monitoring of self-assembly in vitro**
- ✓ **Recognition of amyloids in vivo**
- ✓ **To identify aggregation inhibitor**
- ✓ **Lower cost than PET** (Positron Emission Tomography)
- ✓ **No exposure to radioactivity**

Especially, **ThT** has been used to elucidate the process of aggregate formation.

The mechanism of amyloid recognition

■ W/O amyloid aggregates

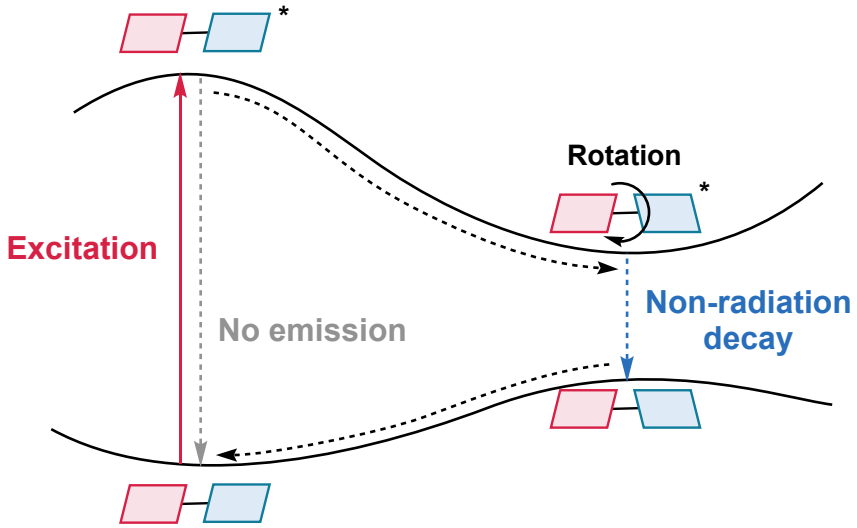

■ W/ amyloid aggregates

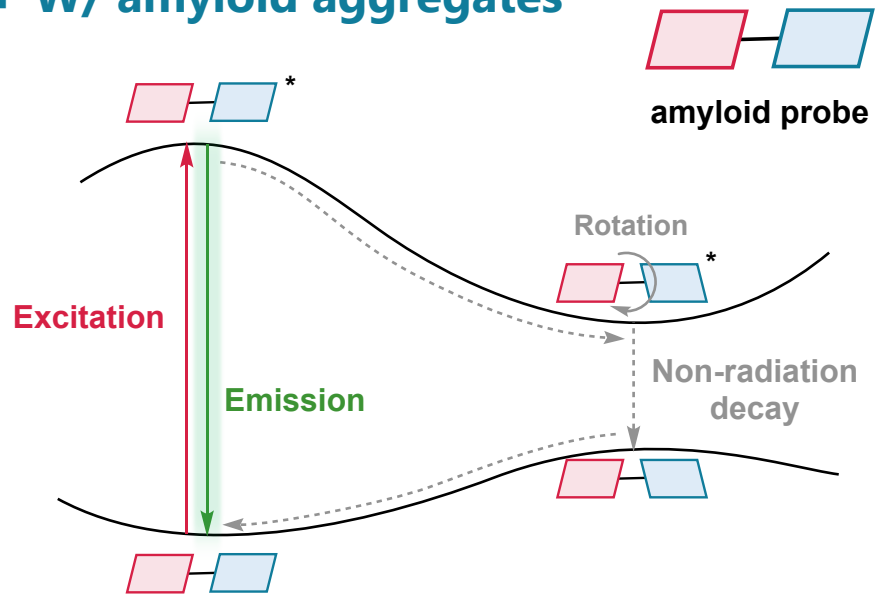

- In the unbound state, **intramolecular rotation causes rapid self-quenching.**
  → **No light emission**

- The presence of amyloid aggregates **restricts the intramolecular rotation**.
  → **The enhancement of fluorescence intensity**

Problems

- It is still **unclear** how amyloid probes bind to fibrils.
- **Heterogeneous structures** of amyloids *in vivo* make it difficult to elucidate their pharmacophore.
- For accurate diagnosis, **protein-selective amyloid probes** need to be developed.

Table of contents

The structure of Aβ fibrils

Fibril structure of Aβ determined by cryo-EM

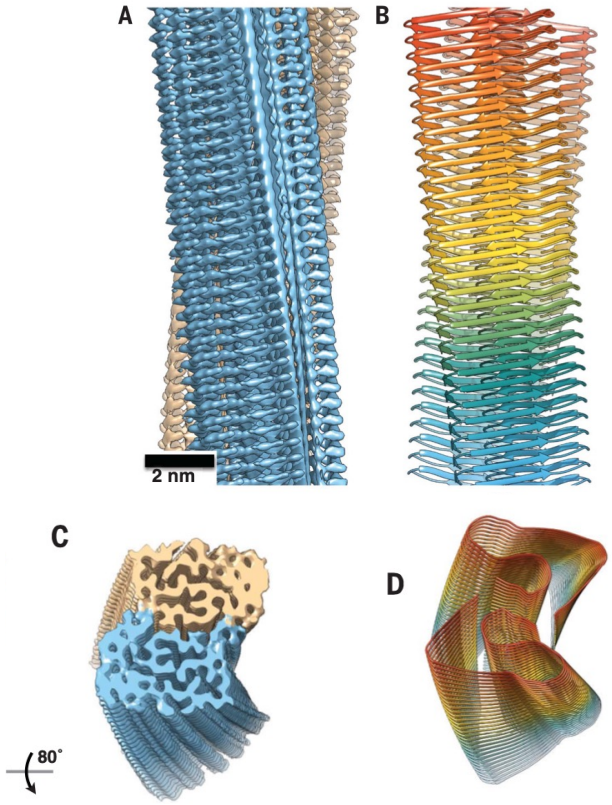

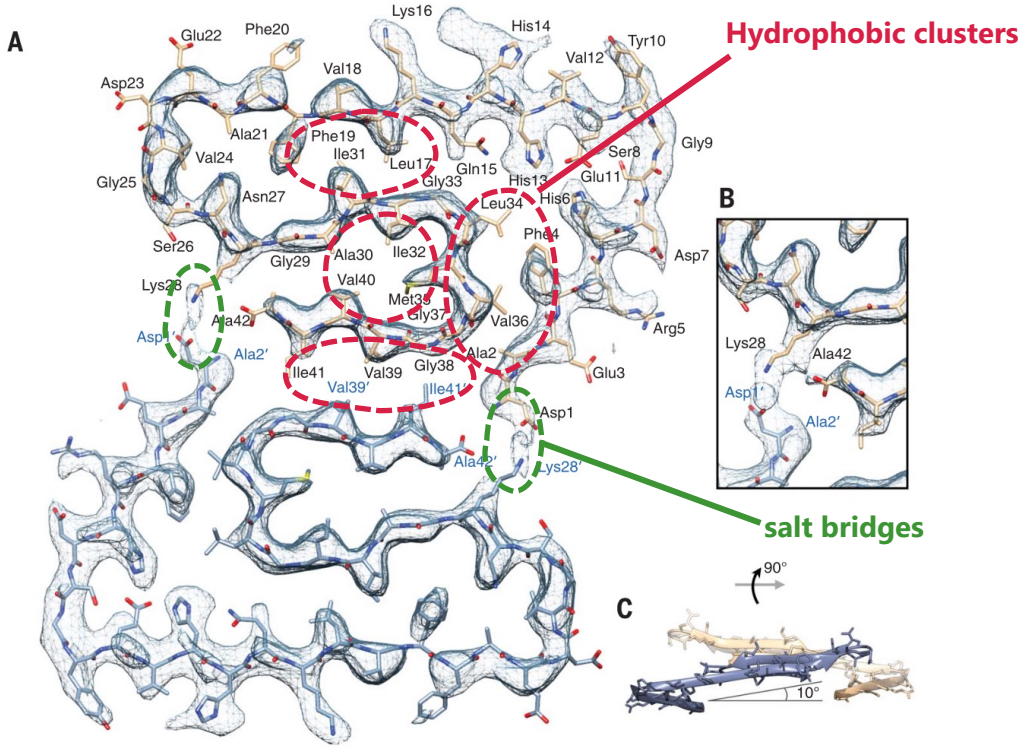

- **Two twisted protofilaments** composed of Aβ(1–42) molecules stacked in a parallel.
- A single Aβ subunit forms an **LS-shaped** structure.

Lother Gremer, *et al. Science*, **2017**, *358*, 116–119.

Binding sites of ThT

- **Multiple binding sites (BSs) of ThT**

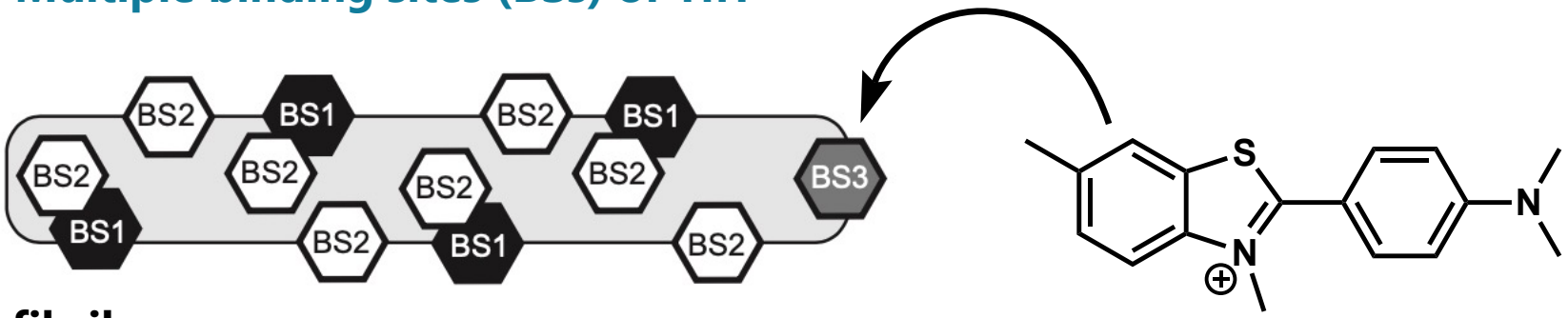

Aβ fibril

Thioflavin T (ThT)

- **BS1 & BS2**
  - **Relatively abundant** (approximately one site per 4-35 monomers)
  - BS1 and BS2 are thought to be in **close proximity** (∵**FRET**).
  - Composed of **surface grooves created by aligned side chains**

- **BS3**
  - **Less abundant** than BS1 and BS2 (approximately one site for 300 monomers)

Ashley A. Reinke and Jason E. Gestwicki, *Chem. Biol. Drug Des*. **2011,** *77*, 399–411.

Binding sites of ThT

- **Two binding channels (molecular docking study)**

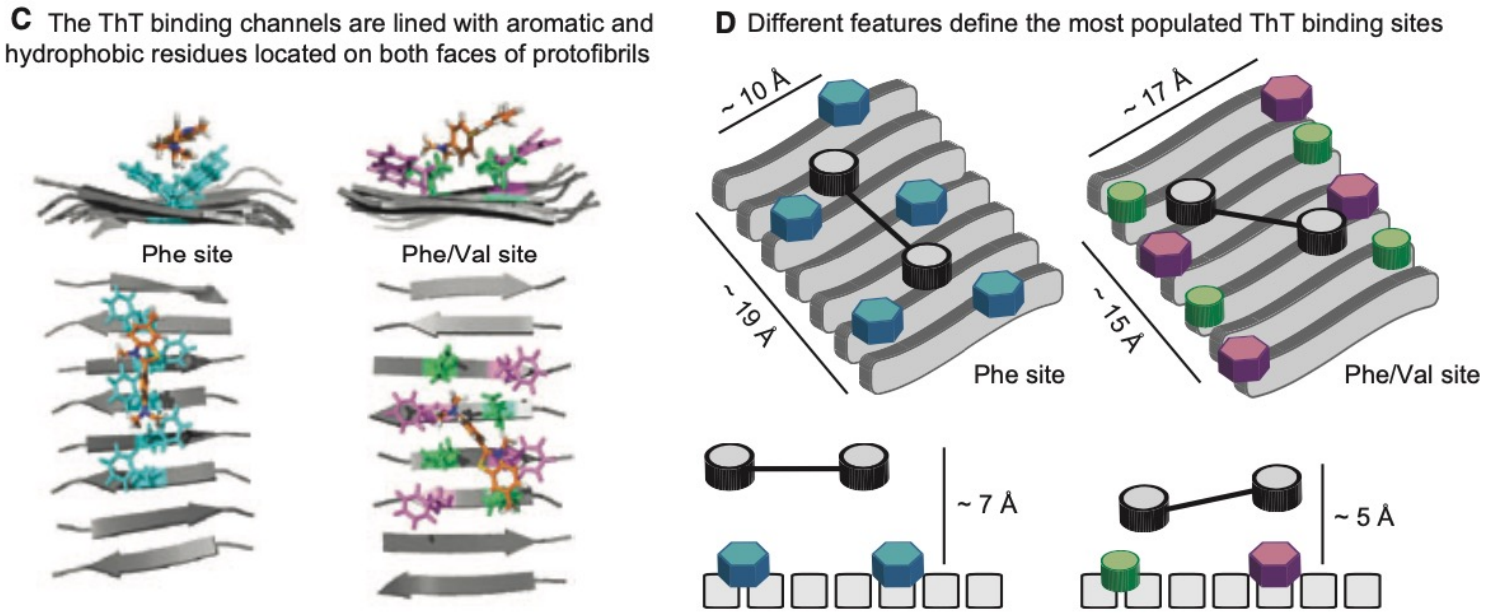

At least five, spatially consecutive, hydrophobic (**Phe only** or **Phe** and **Val**) **side chains** are important.
→ **Hydrophobic interactions and π-π stacking**

(Similar findings have been reported by Dr. Koide and Dr. Makabe)

Ashley A. Reinke and Jason E. Gestwicki, *Chem. Biol. Drug Des*. **2011,** *77*, 399–411.

Binding sites of ThT

- **Two binding channels (molecular docking study)**

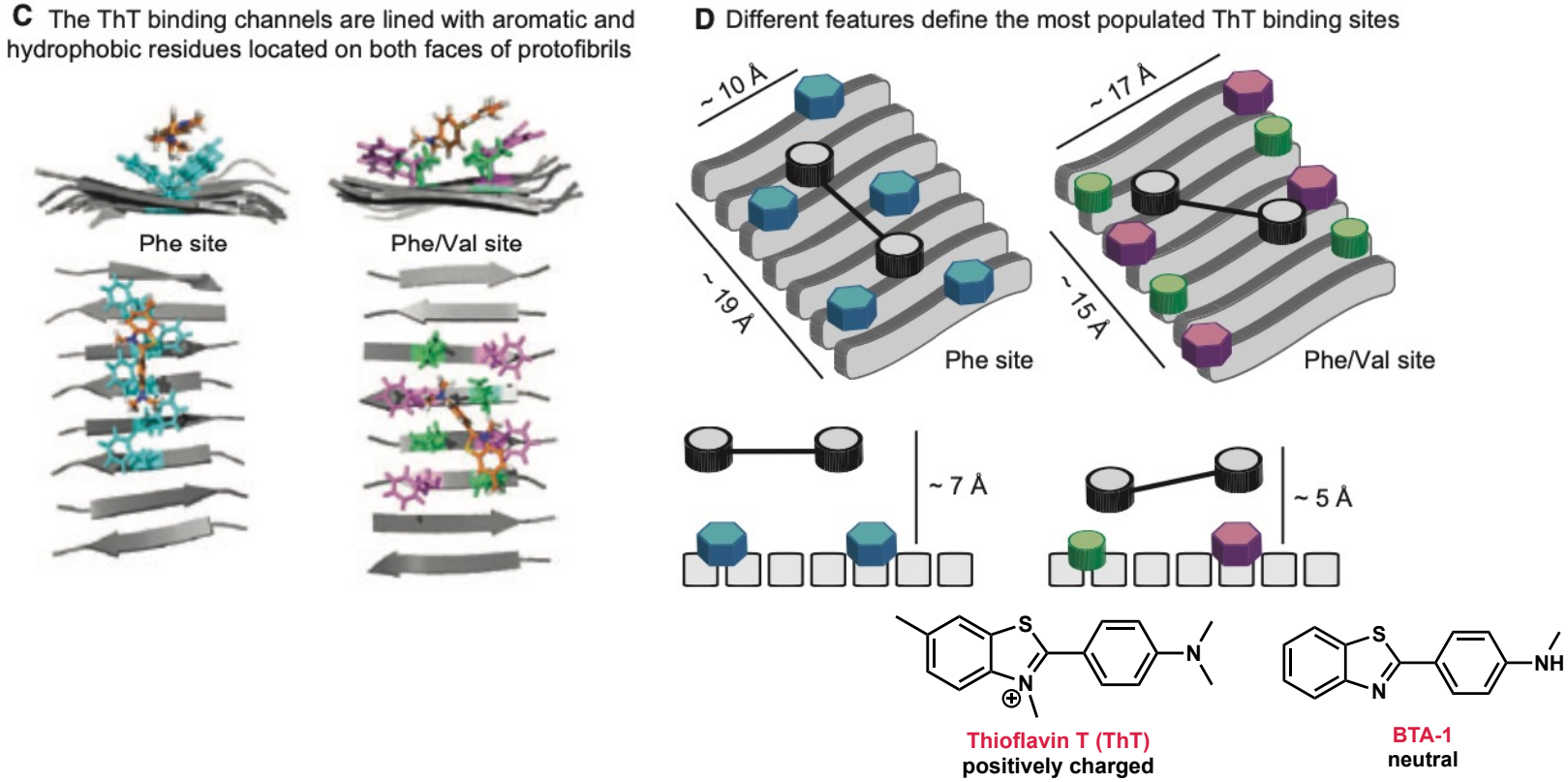

Neutral BTA-1 has much better affinity to A*β* fibrils

→ Neutral molecules can **bind deeper** into the **hydrophobic binding grooves.**

e.g. Phe only site (left) is **deeper and narrower** than Phe/Val site (right).

Ashley A. Reinke and Jason E. Gestwicki, *Chem. Biol. Drug Des*. **2011,** *77*, 399–411.

Binding sites of Congo Red (CR)

- **Multiple binding sites of ThT**

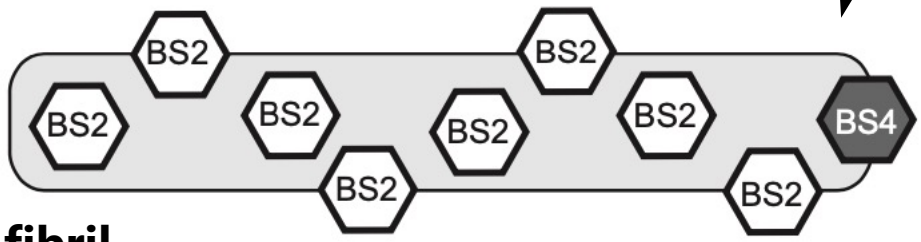

Aβ fibril

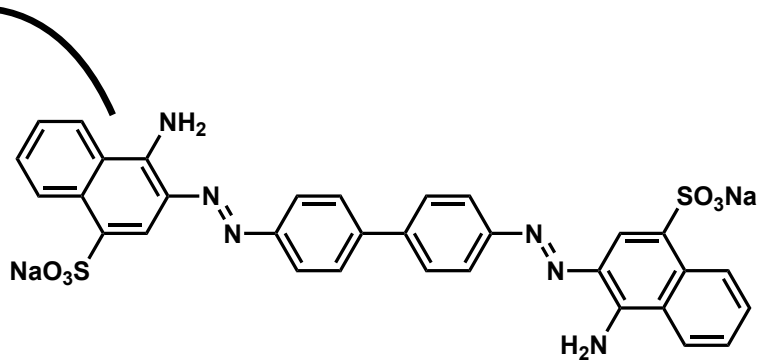

Congo Red (CR)

- **BS2**

  One site per 3 monomers

  Shared by ThT (The competition between ThT and CR was reported.)

- **BS4**

  Unique binding site for CR (Discrete binding sites of ThT and CR was also observed.)

  Lower density

  BS4 may be **at the face of the growing fibril.**

Ashley A. Reinke and Jason E. Gestwicki, *Chem. Biol. Drug Des.* **2011,** *77*, 399–411.

Binding sites of Congo Red (CR)

The binding channel of CR (molecular docking study)

D Charged groups of CR make polar contacts with amyloid fibrils backbone

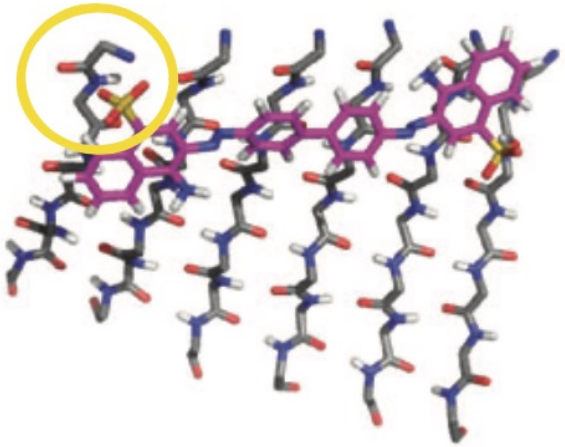

E Polar contacts drive CR binding

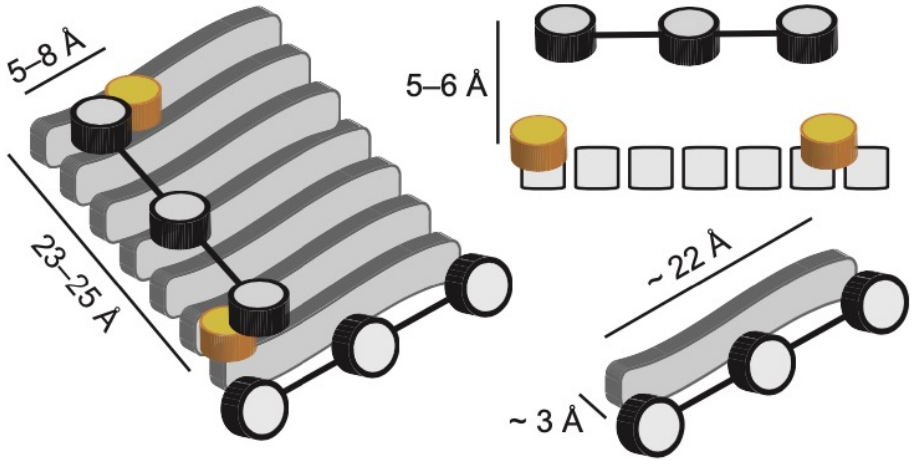

- The CR-binding channel is **longer** and **narrower** than that of ThT.
- The aligned residues are largely **polar and non-aromatic** (such as **Asn** and **Gly**).
  →**Ionic or polar interactions** may be important.

Ashley A. Reinke and Jason E. Gestwicki, *Chem. Biol. Drug Des*. **2011,** *77*, 399–411.

Binding sites of Congo Red (CR)

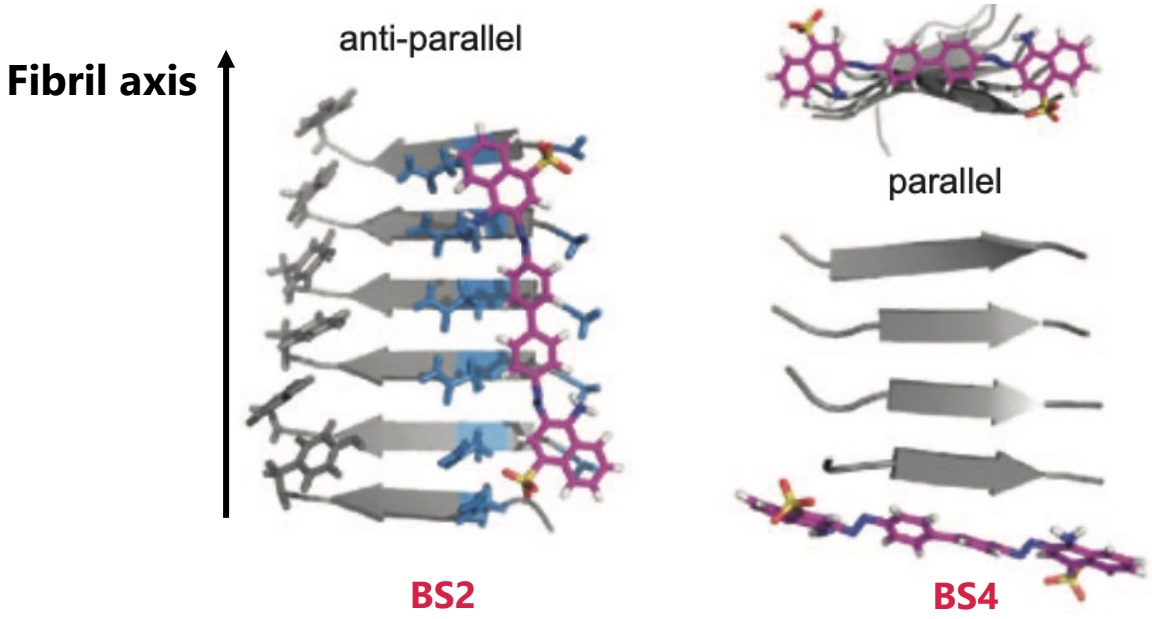

BS2 → Approximately **78 %** of the total CR binding clusters
BS4 → **11 %** of the total binding

↓

An explanation for the difference between CR **binding affinity** (K_d high nM ~ low µM) and its **inhibition capacity** (K_d mid-high µM)

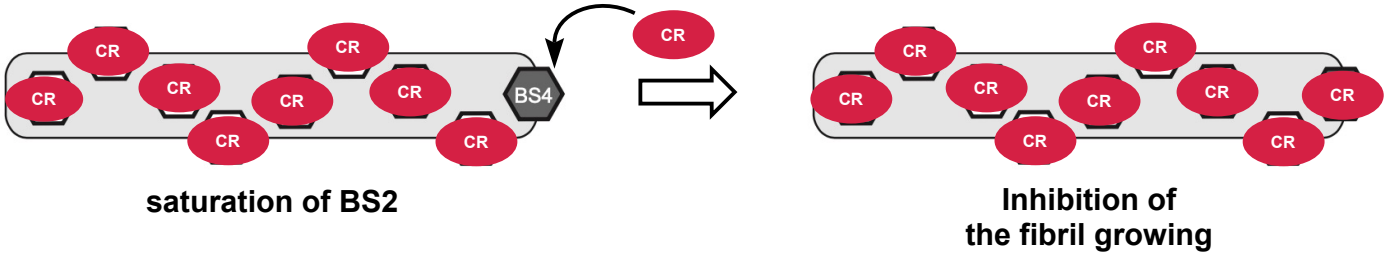

Ashley A. Reinke and Jason E. Gestwicki, *Chem. Biol. Drug Des.* **2011,** *77*, 399–411.

Another example of binding modes

Binding sites of ThT and CR (molecular dynamic simulation)

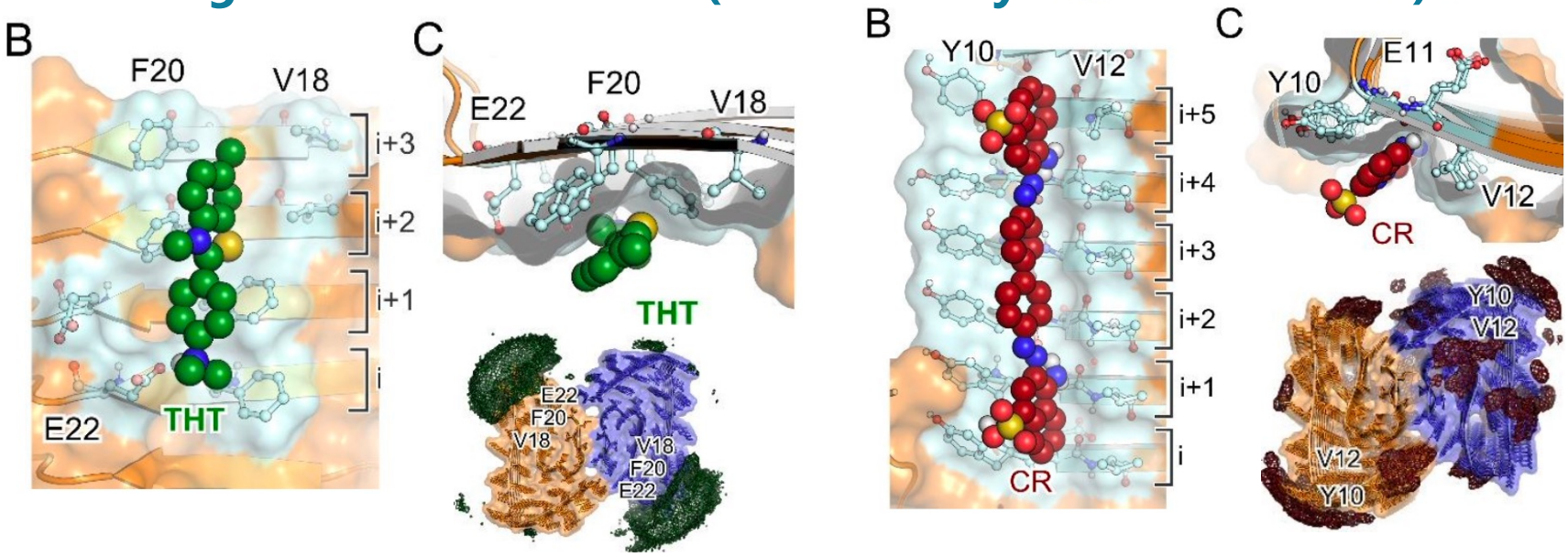

ThT

- ThT binds across **multiple A*β* peptides**, **forming π-π stacking with F20**.
  → It recognizes only A*β* fibrils (not single A*β*).

CR

- CR binds to the groove between **Y10** and **V12** forming edge-to-face **aromatic** and **hydrophobic interactions.**
- Carbonyl oxygen → Forming **hydrogen bond** with **E11**
- Sulfonate group → **Exposed to the solvent**

Frieg, B, Lother Gremer, *et al. Chem. Commun.* **2020**, *56* (55), 7589– 7592.

Table of contents

Selective detection for Aβ oligomers

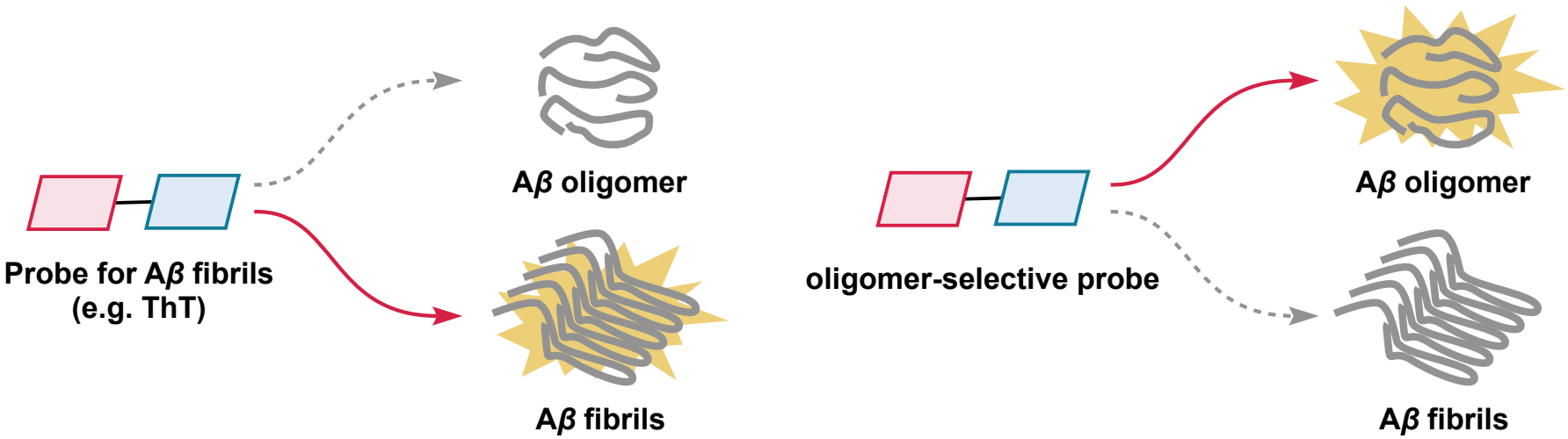

- **Oligomeric soluble Aβ** is responsible for the pathogenesis of Alzheimer's disease.
- There are a number of fibril-specific dyes but **few dyes which preferentially recognize Aβ oligomers**.
- It is necessary to develop **oligomer-selective small fluorescent molecular probes.**

Chai Lean Teoh *et al. J. Am. Chem. Soc*. **2015**, *137*, 13503−13509.

Selective detection for Aβ oligomers

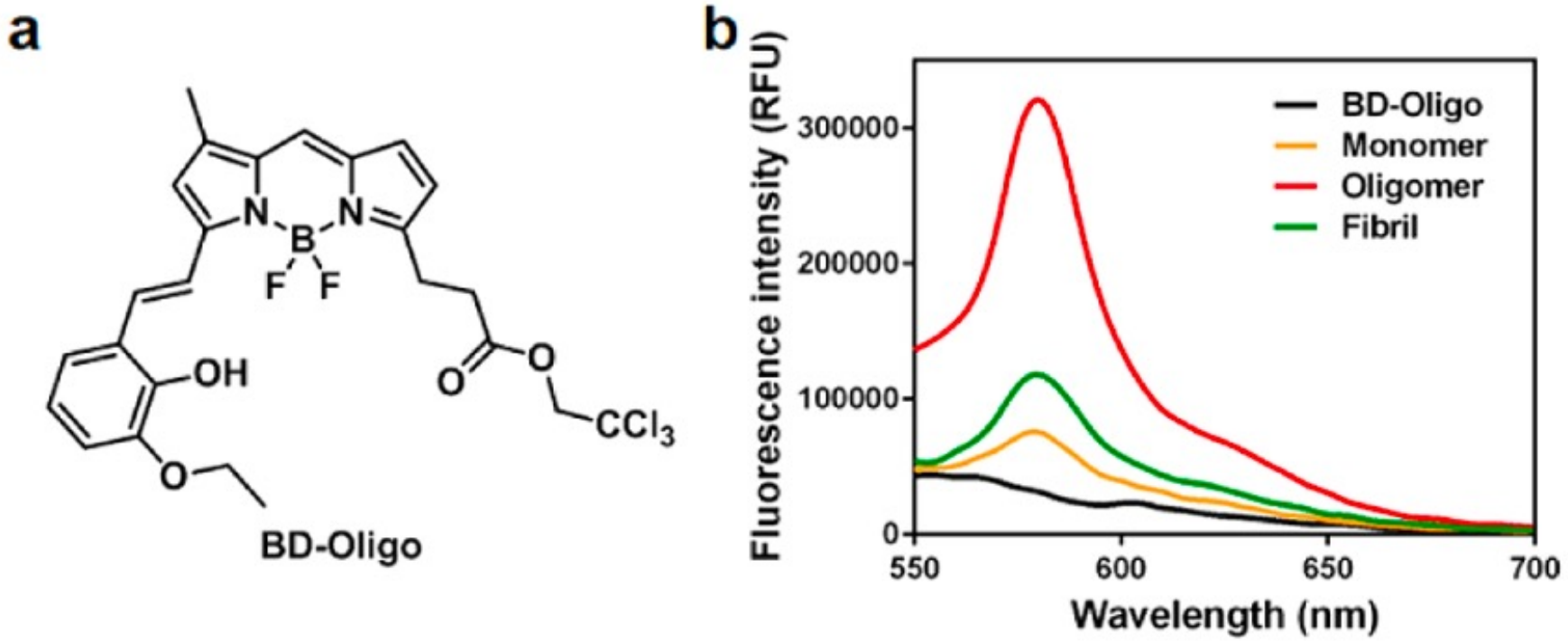

The highest fluorescence enhancement with Aβ oligomers

↓

BD-Oligo preferentially recognizes Aβ oligomers over monomers or fibrils

Chai Lean Teoh *et al. J. Am. Chem. Soc*. **2015**, *137*, 13503−13509.

Selective detection for Aβ oligomers

ThT & BD-Oligo

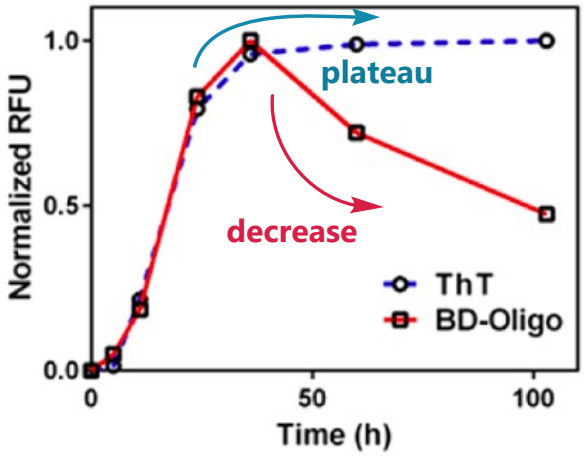

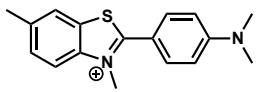

Thioflavin T (ThT)
Aβ aggregates selective

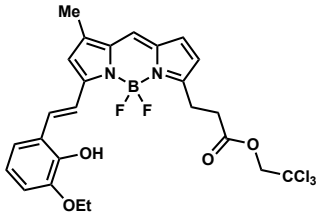

BD-Oligo
Aβ oligomer selective

Pelleting assay

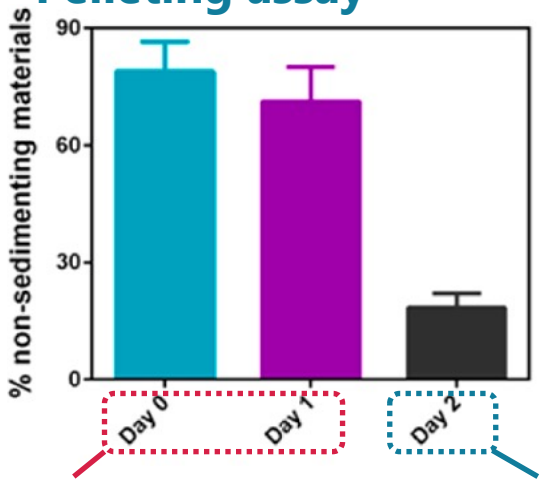

The majority of Aβ is still in solution

Aβ starts to form a large segmenting materials

TEM images

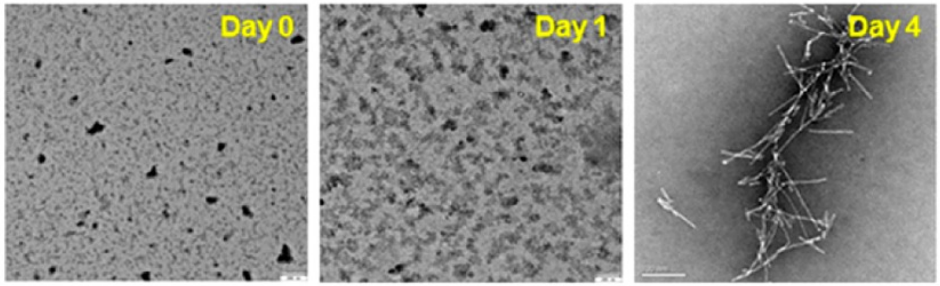

Day 0 and Day 1: **No sign of fibrils**

Day 4: **Fibril formation** was observed.

The presence of β-sheet structure alone does not suffice to explain the binding specificity of BD-Oligo.

↓

What is the structural feature of Aβ oligomers?

Chai Lean Teoh *et al. J. Am. Chem. Soc*. **2015**, *137*, 13503−13509.

A working model of Aβ oligomers

The structure of the mimic of $A\beta_{17-36}$ trimer

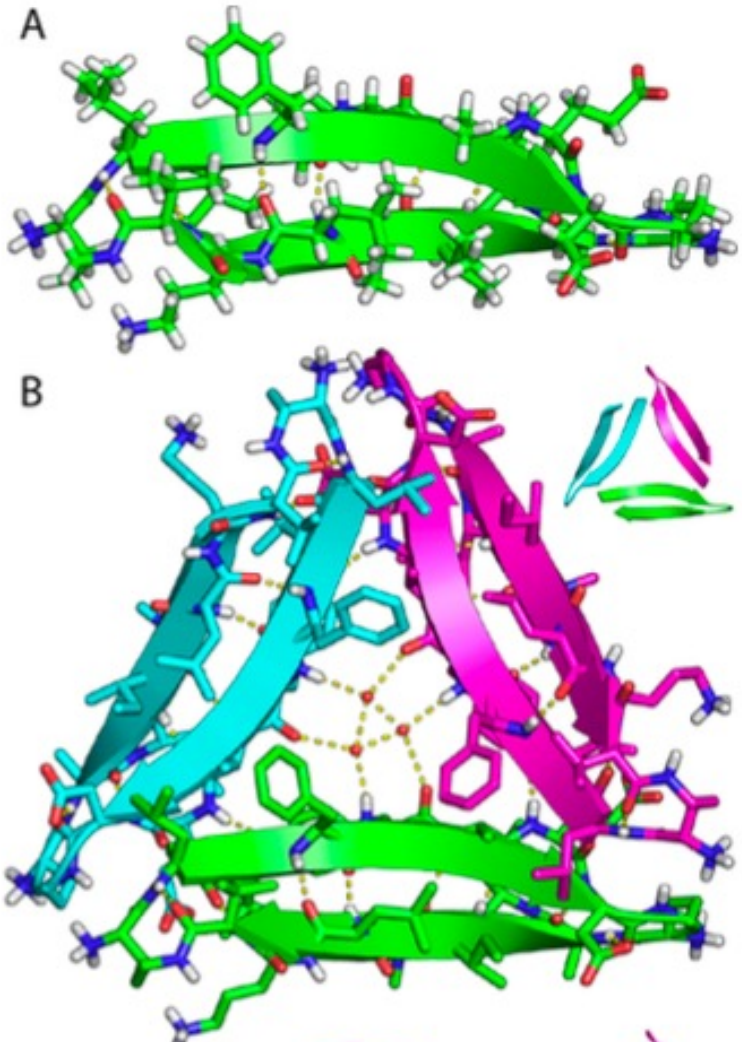

Structural features of Aβ trimer

- ✓ The trimer consists of **three twisted β-hairpins.**
- ✓ Phe19 and Val36 form **hydrophobic patches** at the center of Aβ trimer.

Importantly, these hydrophobic patches are exposed only in Aβ oligomers but not in Aβ fibrils (oligomer-specific).

Ryan K. Spencer, Hao Li, and James S. Nowick, *J. Am. Chem. Soc.* **2014**, 136, 5595−5598.

A working model of Aβ oligomers

- **The structure of the mimic of $A\beta_{17-36}$ trimer**

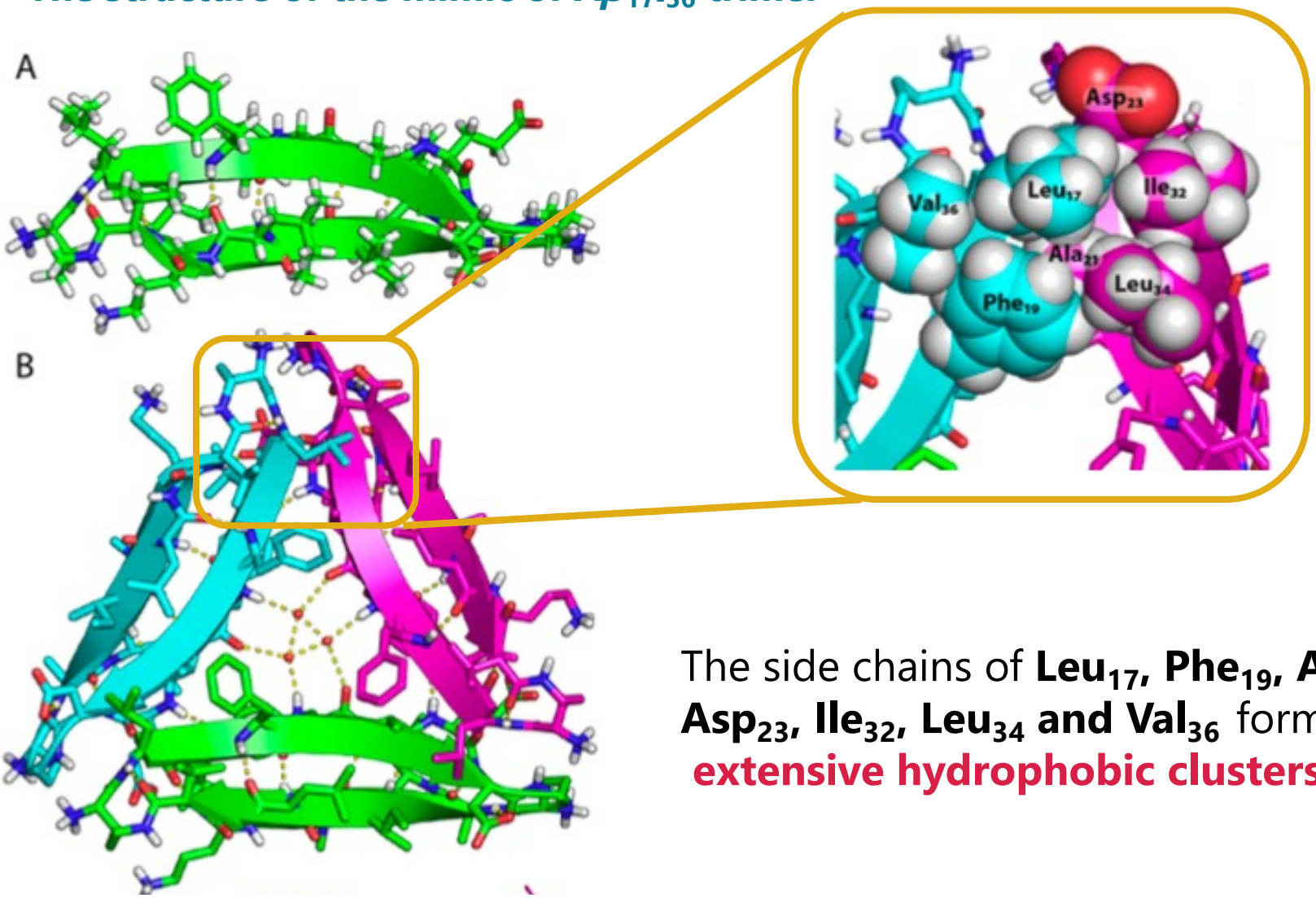

The side chains of **Leu_{17}, Phe_{19}, Ala_{21}, Asp_{23}, Ile_{32}, Leu_{34} and Val_{36}** form **extensive hydrophobic clusters**.

Ryan K. Spencer, Hao Li, and James S. Nowick, *J. Am. Chem. Soc.* **2014**, 136, 5595−5598.

Molecular docking using working model

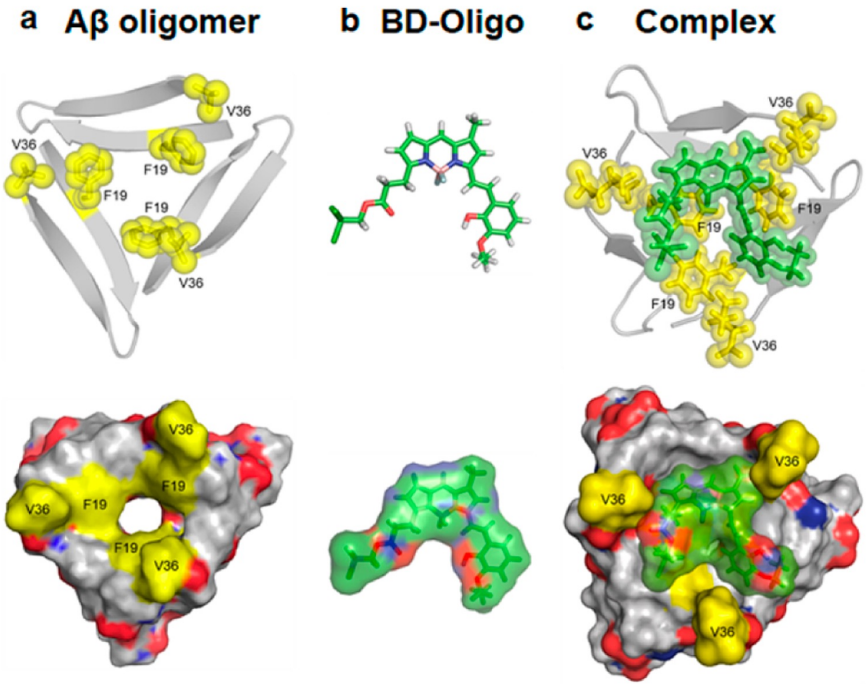

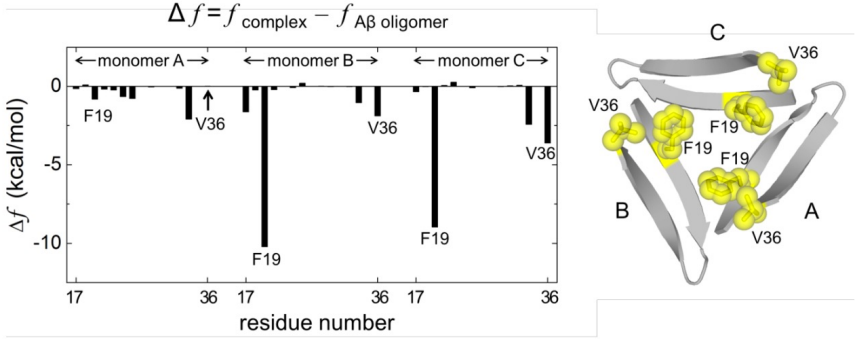

Site-directed thermodynamics analysis of the BD-Oligo complex with A*β* oligomer (Aβ17-36)

BD-oligo recognizes F19 and V36 in A*β* oligomers.

- **Hydrophobic patches (F19)**
  π-π stacking with aromatic ring od BD-oligo
- **V36**
  Hydrophobic interaction / **CO---H bonding** with carbonyl group of BD-oligo

Chai Lean Teoh *et al. J. Am. Chem. Soc*. **2015**, *137*, 13503−13509.

Ex vivo binding of BD-Oligo in AD mouse brain

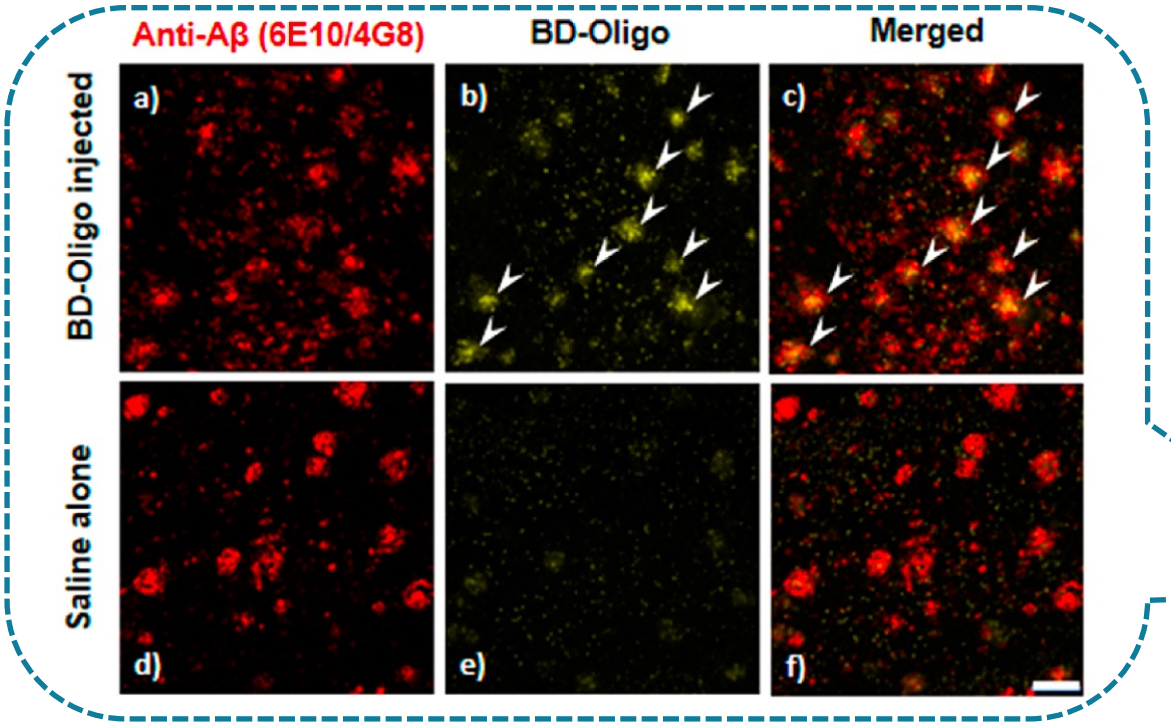

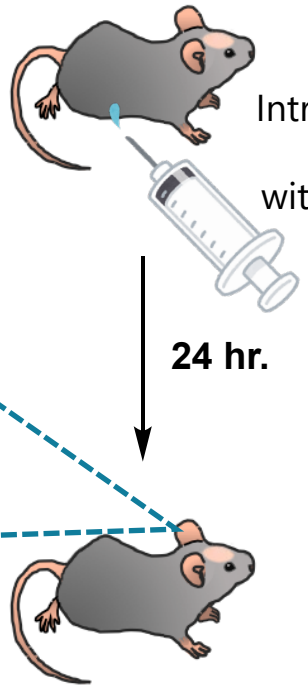

***Ex vivo* imaging**

BD-Oligo labeling not only appeared in the **central core of A*β* plaques** but was also present in **the periphery of plaques**.

↓

This result reflects the hypothesis that **A*β* plaque may function as a reservoir for soluble oligomers.**

Chai Lean Teoh *et al. J. Am. Chem. Soc*. **2015**, *137*, 13503−13509.

Other examples of Aβ oligomer probes

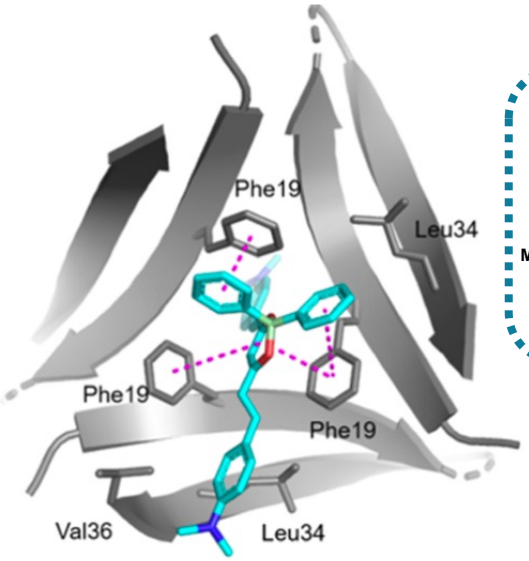

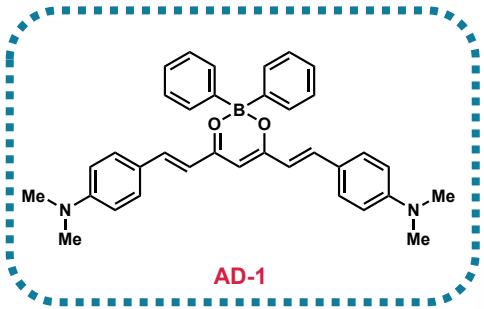

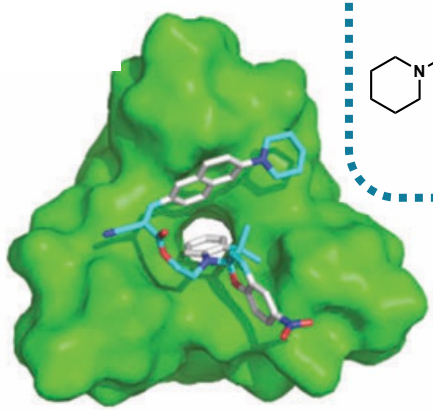

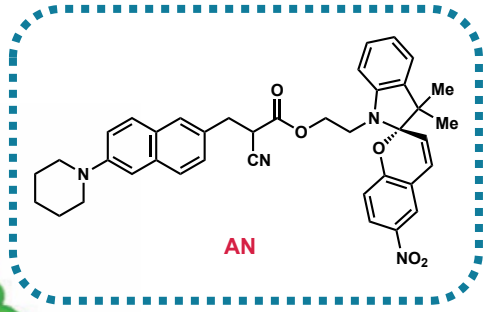

*AD-1 also recognizes Aβ monomers and aggregates

The main binding mode is the **π-π stacking interactions** between **Phe 19** and **aromatic rings** of probes.

Their twisted structures may affect the binding affinity to oligomers ??

left: Yiran Ge *et al. ACS Chem. Neurosci.* **2021**, *12*, 19, 3683–3689.
right: Guanglei Lv *et al. Chem. Commun.*, **2016**, *52*, 8865-8868.

Table of contents

Difficulties in developing tau-selective probes

- Common β-sheet structure
- The lack of clear pharmacophore
- The structural diversity of tau proteins
- PTMs (Post-Translational Modification)

↓

Rational design of tau-selective probes is difficult…

However, there are **two hypotheses** to guide the molecular design of tau binders.

Two hypotheses

1. **A distance of 13 to 19Å between the donor and acceptor parts benefits tau selectivity.**

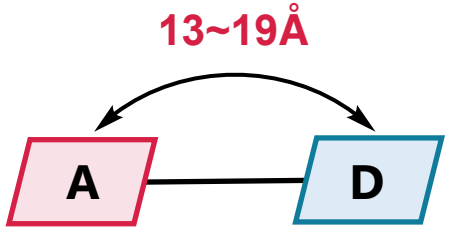

→ **Tau selective detection**

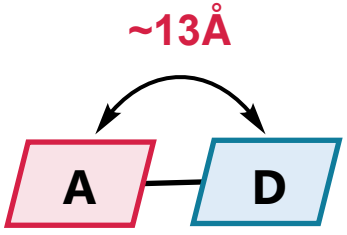

→ **Shorter distance favors Aβ plaques**

2. **Dyes containing fused ring system tend to have tau selectivity over Aβ fibrils.**

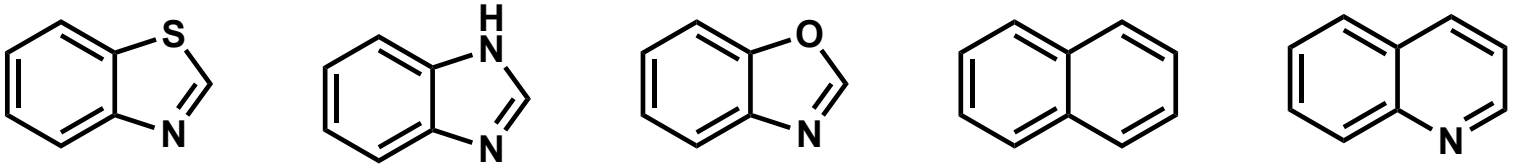

Examples of fused ring system

Ariza,M. *et al. J. Med. Chem.* **2015**, 58, 4365−4382.
Maruyama M. *et al. Neuron,* **2013**, 79, 1094−1108.
Peter Verwilst *et al. J. Am. Chem. Soc.* **2017**, 139, 13393−13403.

New tau-selective probes

Tau 1 & Tau 2: Rationally designed probes

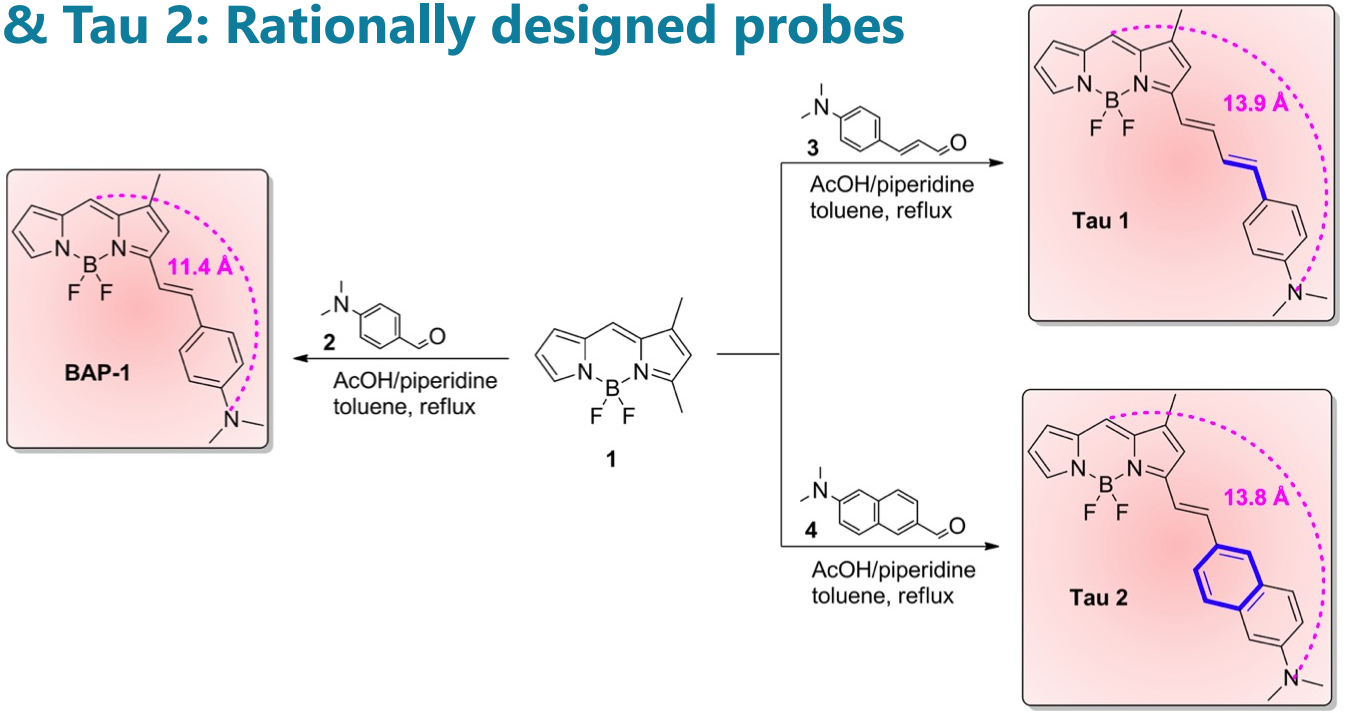

- ✓ **About 14Å between donor and acceptor**
- ✓ **Fused ring system**
- ✓ → More likely to interact with the β-sheet fibrillar aggregates present in PHF-tau
- ✓ **Short synthetic route**
- ✓ **Tau selective detection *in vitro* and *in vivo***

Peter Verwilst *et al. J. Am. Chem. Soc.* **2017**, 139, 13393−13403.

Selective responses to Tau aggregates

Tau

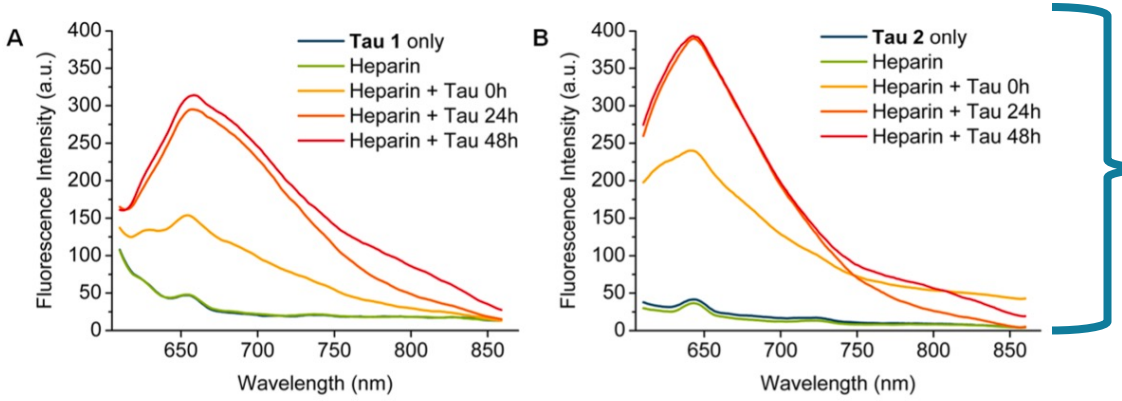

w/ tau aggregates

- ✓ No significant fluorescence in heparin only
- ✓ Time-dependent **fluorescent enhancement**

Aβ

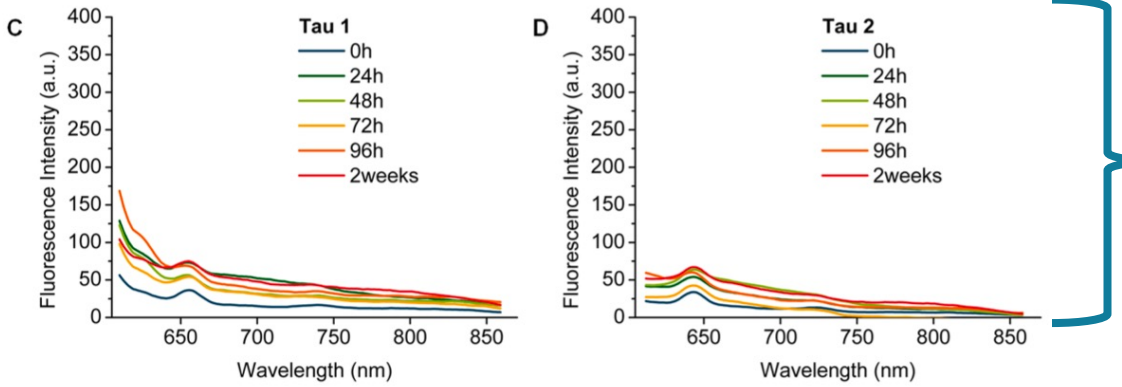

w/ Aβ aggregates

- ✓ **Trivial responses** to the presence of Aβ aggregates

Tau 1&2 are highly selective to Tau protein aggregates over Aβ aggregates

Peter Verwilst *et al. J. Am. Chem. Soc.* **2017**, 139, 13393−13403.

In cell assay

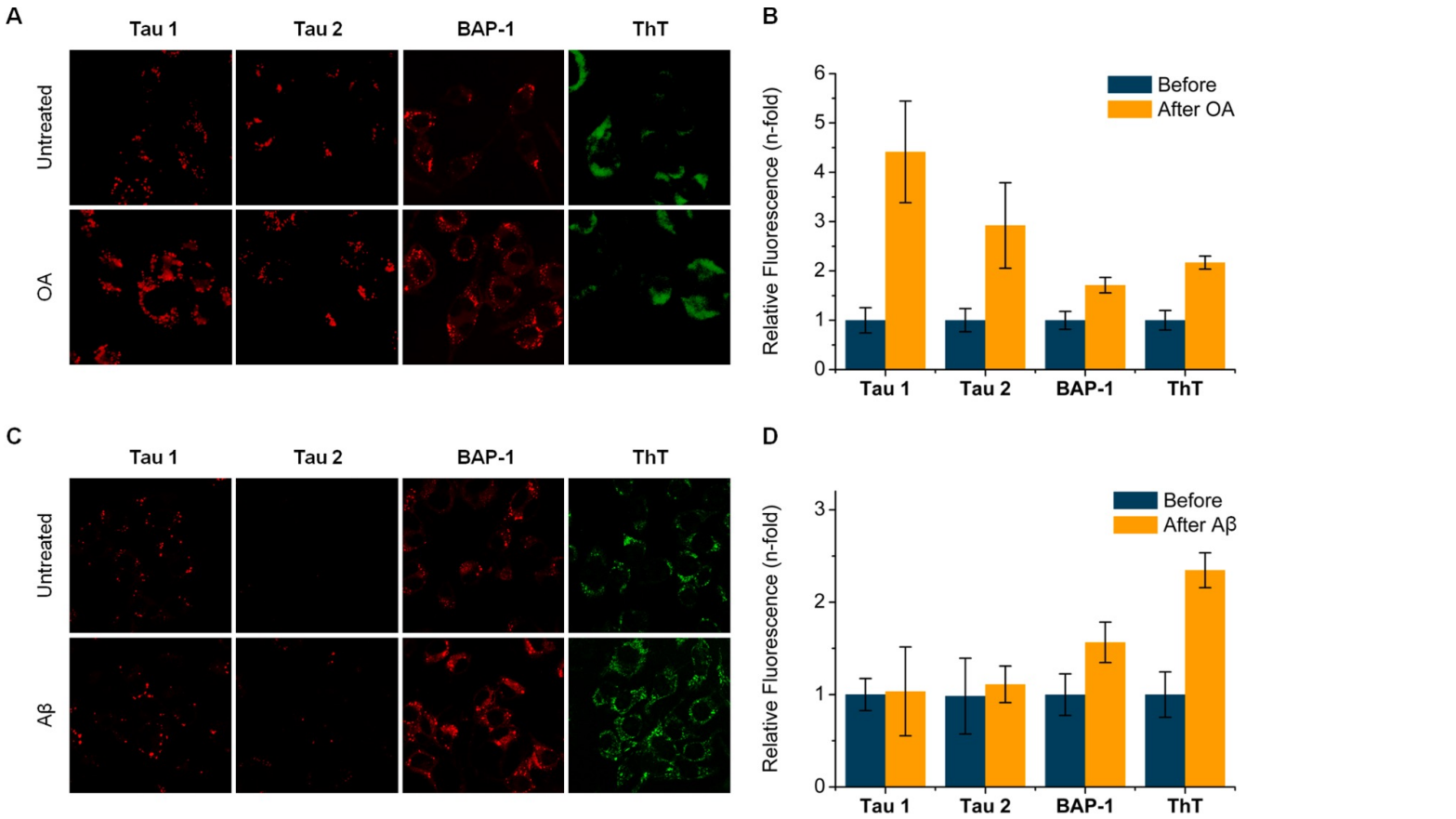

*OA: Okadaic acid(an inhibitor of phosphatases) → ***In vitro* tau hyperphosphorylation model**

Both of two probes (especially **Tau 1**) are capable of detecting **hyperphosphorylated tau aggregates selectively over A*β* aggregates even in cellular environments.**

Peter Verwilst *et al. J. Am. Chem. Soc.* **2017**, 139, 13393−13403.

Ex vivo imaging of Tau 1

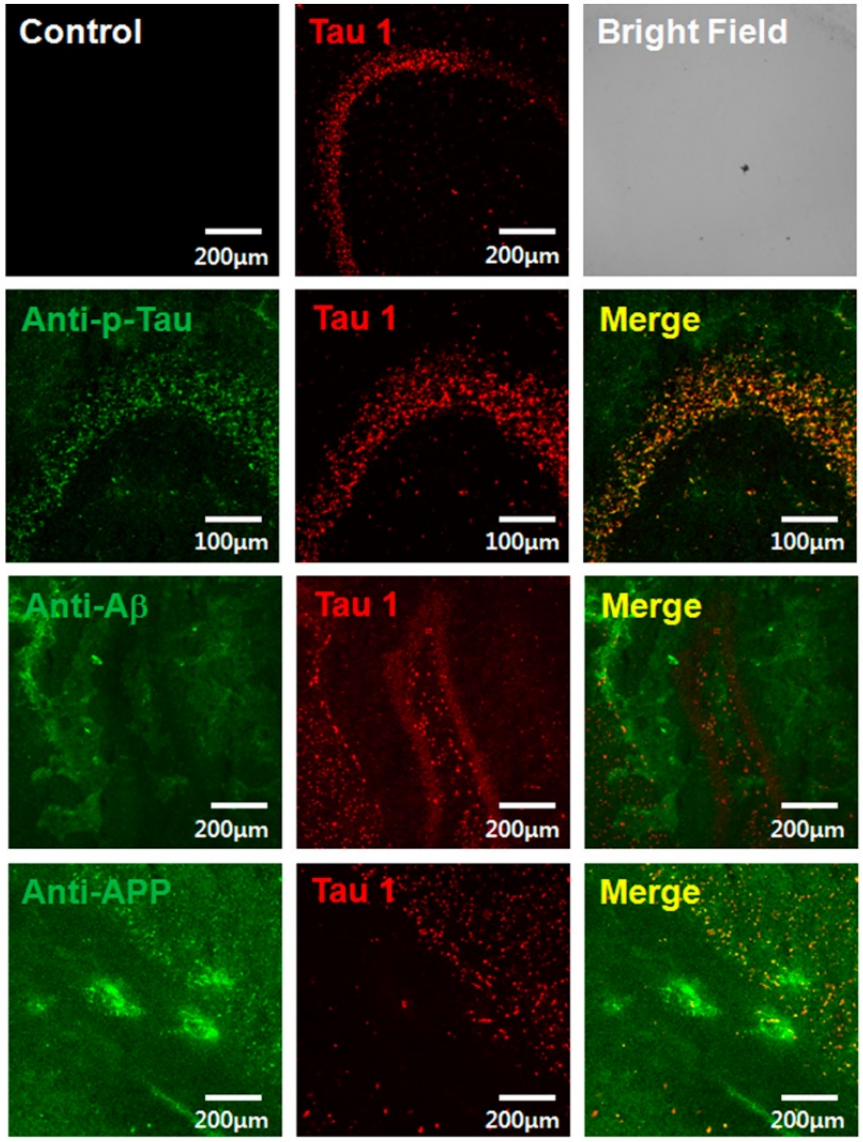

Intracranially injected with Tau 1

✓ **Anti tau and Tau 1**
→**a very high degree of overlap**

✓ **Anti Aβ / APP and Tau 1**
→**virtually no overlap**

Tau 1 co-localized with tau but not with A*β* under these conditions

Peter Verwilst *et al. J. Am. Chem. Soc.* **2017**, 139, 13393−13403.

In vivo imaging of Tau 1

Protocol

Excitation at 670 nm **Detection at 699 nm**

Tail vein injection with **Tau 1**

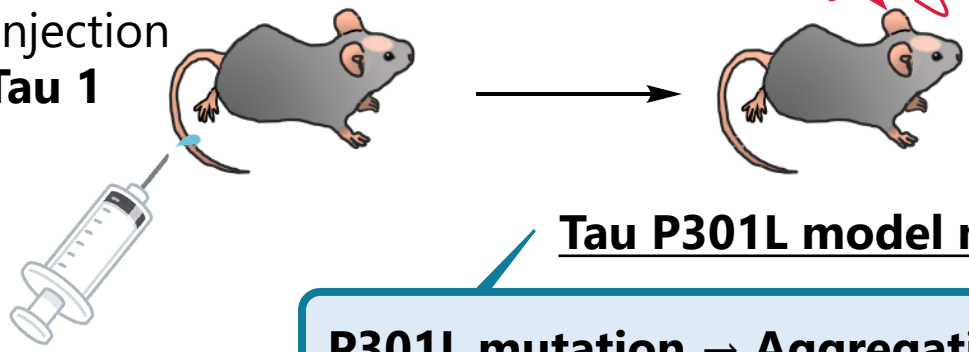

Tau P301L model mouse / WT

P301L mutation → Aggregation-prone tau protein

Result

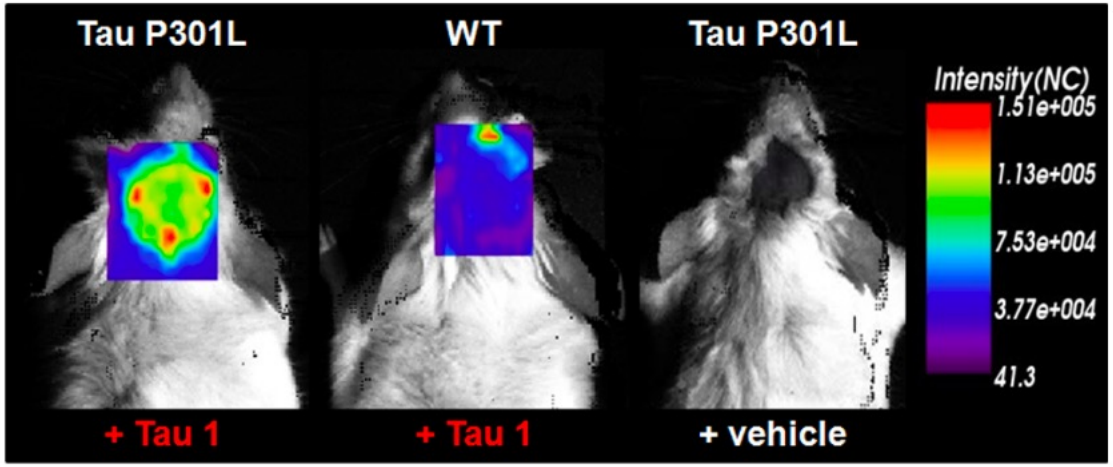

Peter Verwilst *et al. J. Am. Chem. Soc.* **2017**, 139, 13393−13403.

A significantly enhanced fluorescence in the transgenic mouse model

↓

Tau 1 can detect the presence of tau tangles in mice !!

PHF fragment (^{306}VQIVYK^{311})

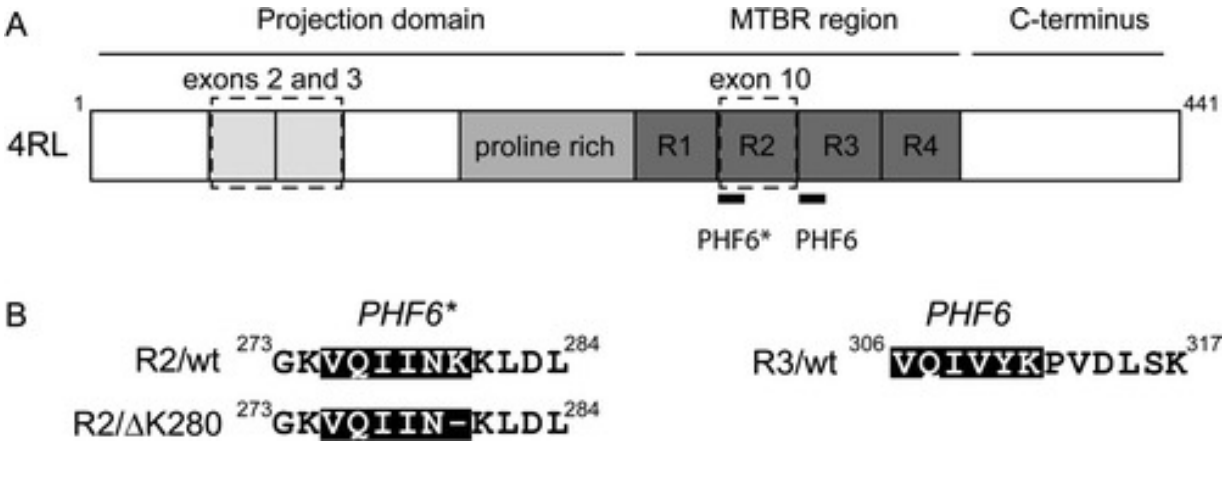

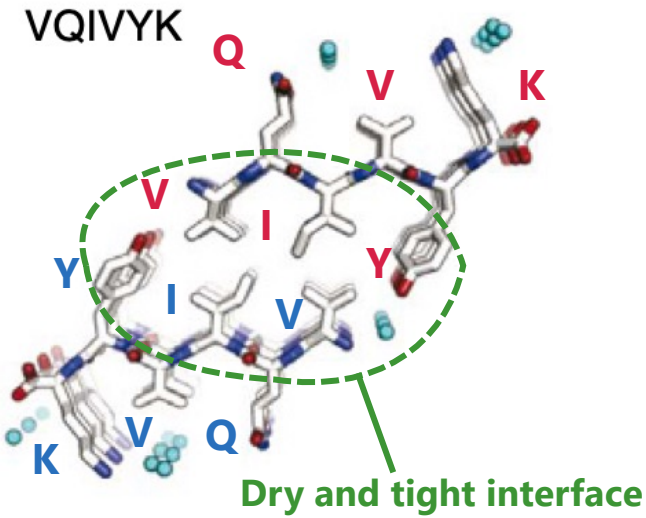

- **PHF sequence** has been demonstrated to play a **pivotal role in the aggregation of tau protein.**
- The crystal structures of **VQIVYK peptide** consists **the steric zipper structure**.
- Co-crystallization with some compounds reveals **a propensity to generate tunnels along the fibril axis (See next page).**

M. von Bergen *et al. PNAS*, **2000**, *97* (10), 5129-5134.
Meytal Landau *et al. PLoS Biol*. **2011**, *9,* 1–13.

Co-crystallization with dyes

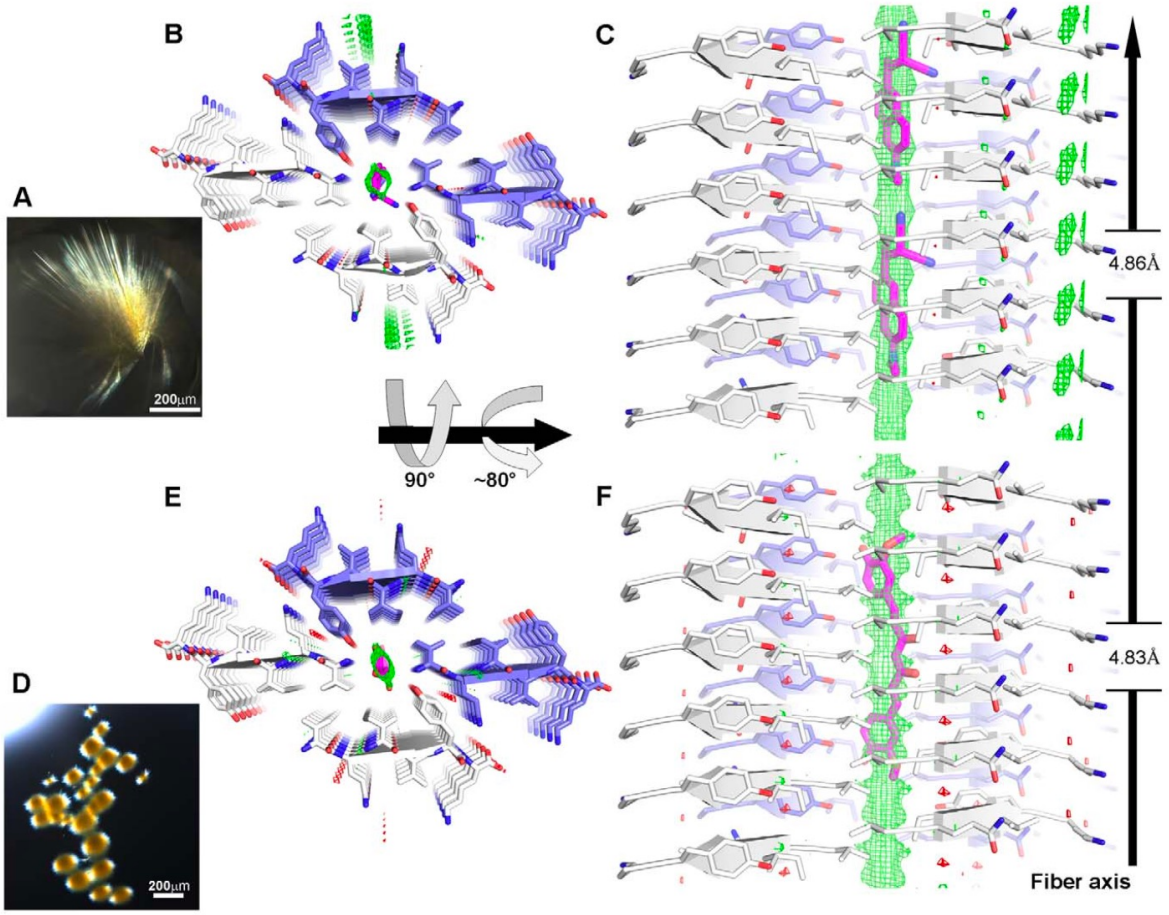

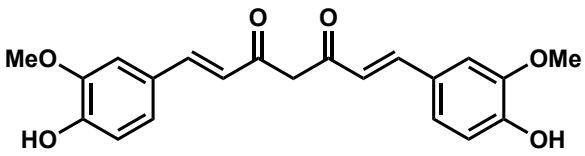

curcumin

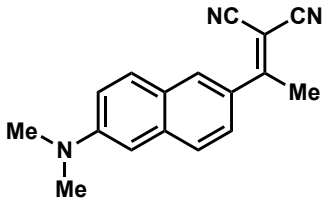

DDNP

These dyes bind to the *β*-sheets with their long axes parallel to the fiber axis.

Meytal Landau *et al. PLoS Biol*. **2011**, *9*, 1–13.

Co-crystallization with dyes

- **Crystal structure (DDNP)**

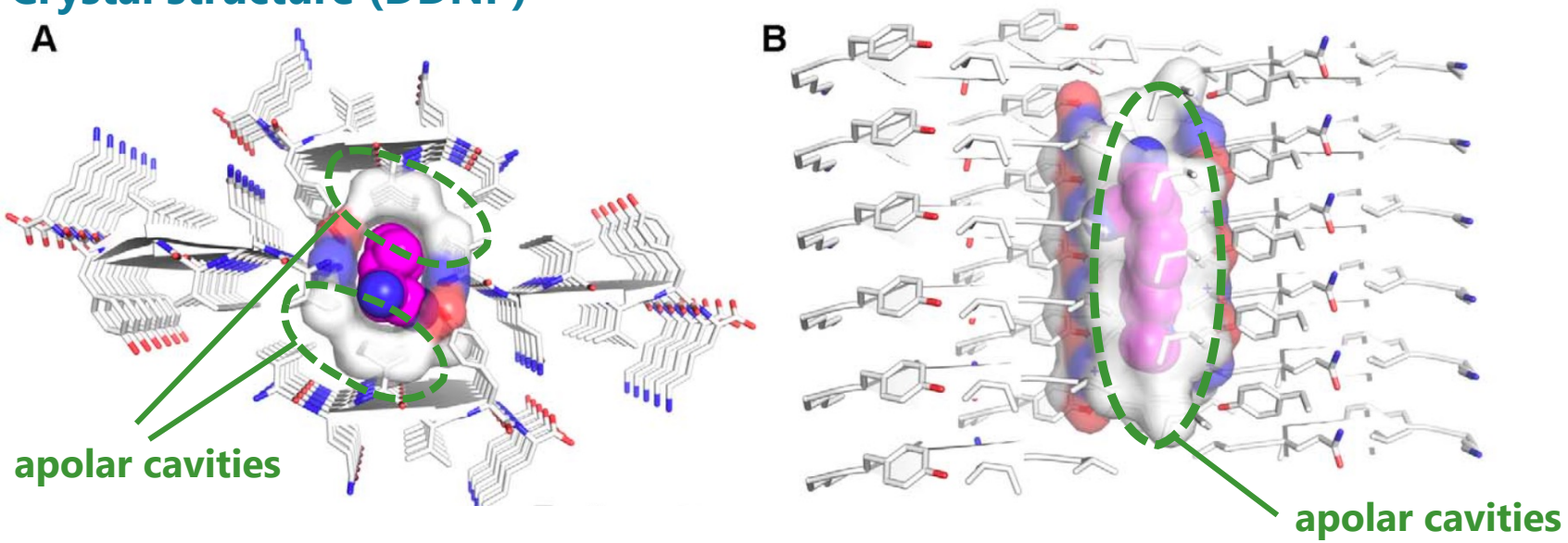

The atomic groups lining the tunnel are about half **apolar** (colored in white) and half **polar** (colored in red and bleu).

↓

This cylindrical, partially apolar structure favors various apolar or aromatic compounds.

These cavities also provide biding sites of apolar drugs (benzodiazepines and anesthetics etc.)
→ An explanation for **the altered pharmacokinetic properties** and **increased sensitivity** in elderly patients ??

Meytal Landau *et al. PLoS Biol*. **2011**, *9*, 1–13.

Molecular docking studies (Tau 1)

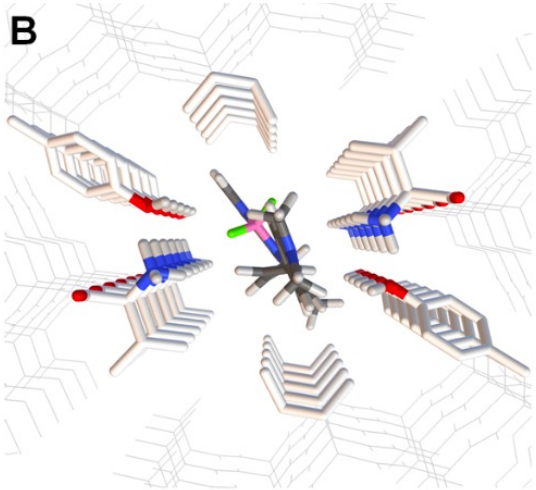

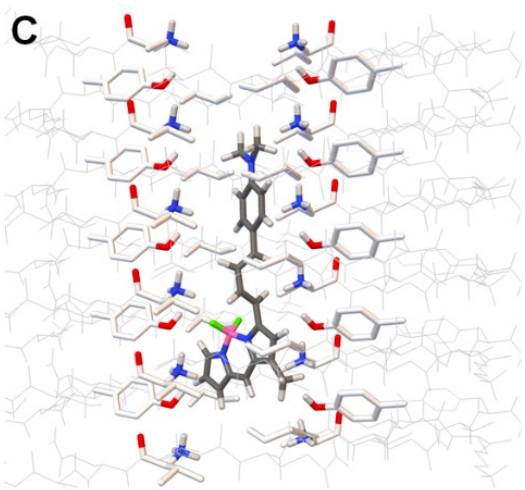

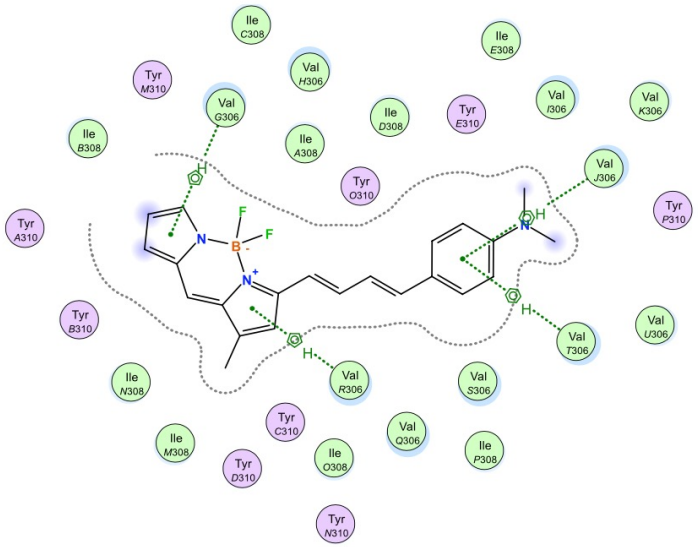

Tau 1 demonstrated a **tight fit** in the tunnel.

The main binding mode is the **hydrophobic interactions** between **aromatic rings of Tau1** and **side chains of Val** .

Peter Verwilst *et al. J. Am. Chem. Soc*. **2017**, 139, 13393−13403.
Ahmed A. Elbatrawy *et al. ACS Sens*. **2021**, *6*, 2281-2289.

Molecular docking studies

Binding affinity of tau-selective probes

Name	Structure	Docking affinity (kCal/mol)
F-ATPZ-38	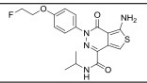	-5.0
BAP-1	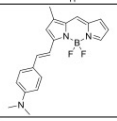	-7.1
Astemizole	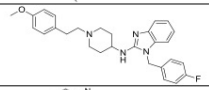	-7.4
I-PDB3	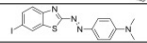	-7.6
FDDNP	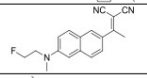	-7.7
PBB5	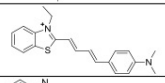	-7.7
BF-188	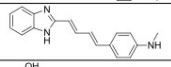	-7.8
S-F-THK-5117	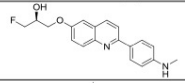	-7.8
Tau 1	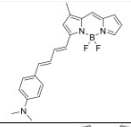	-7.8
F-T808	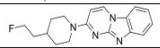	-7.9
F-T807	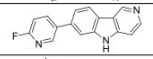	-8.5
Methyl-Lansoprazole	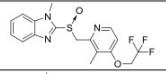	*L*: -8.5 *D*: -8.7
3h	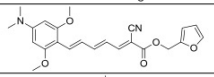	-8.6
Tau 2	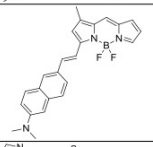	-8.6
I-TH2	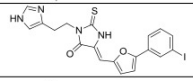	-8.9
N-(2-methoxyphenyl)-*N*'-[4-(1-methyl-1*H*-pyrrolo[2,3-*c*]pyridin-3-yl)phenyl]urea	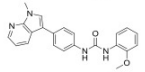	-9.3
F-SKT04-137		-9.3

- Lower binding affinity of BAP-1→ Due to its **smaller surface area** ?
- F-ATPZ-38 & astemizole → Favorable to interact with **other topologies** ?

Peter Verwilst *et al. J. Am. Chem. Soc.* **2017**, 139, 13393−13403.

Table of contents

Summary

- The binding mode of amyloid probes has been **well studied** by utilizing **molecular docking simulation** or **molecular dynamics simulation**.

- These studies provide insights into the **pharmacophore** and keys to the **rational design** of amyloid probes.

- However, these findings need to be interpreted **with caution** as **the exact structures of amyloid fibrils (or oligomers)** ***in vivo*** are **still unclear.**

Thank you for your listening !!

APPENDIX

Molecular docking simulation

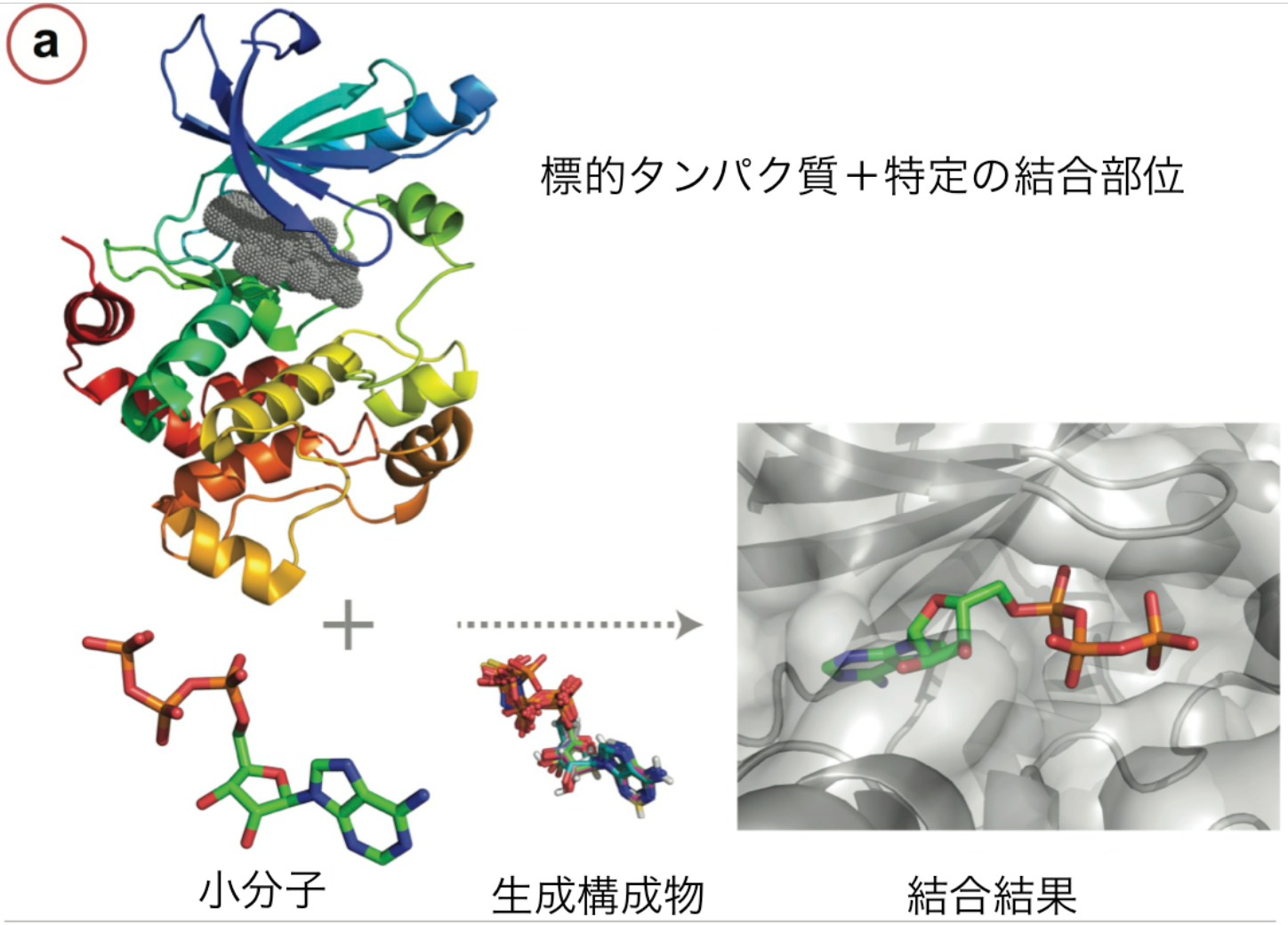

*結合部位があらかじめ定められている場合に有効
(今回取り扱った各文献では、結合部位を想定した上でMDが行われている)

OISTのウェブサイトより: https://www.oist.jp/ja/news-center/photos/14053

Molecular dynamics simulation

Molecular Dynamics

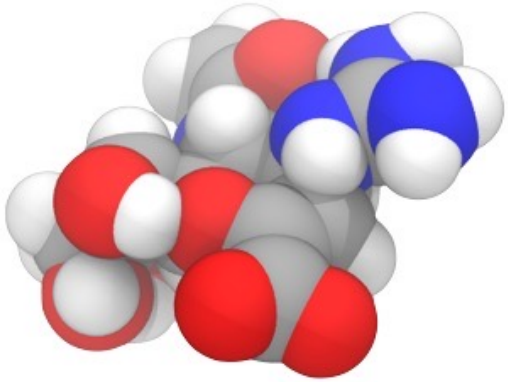

1. Assign velocities to all atoms
2. Calculate forces on all atoms
3. Use Newton's second law to calculate acceleration on each atom

$$F = ma$$

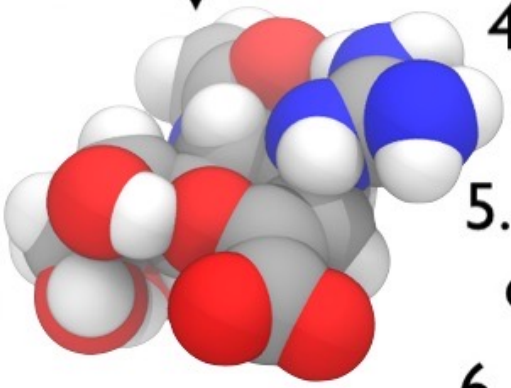

4. Calculate velocities for the next timestep
5. Use change of velocities to get coordinates for next timestep
6. Go to step 2.

http://guillefix.me/cosmos/static/Molecular%2520dynamics.html

Detailed structure of Aβ fibril

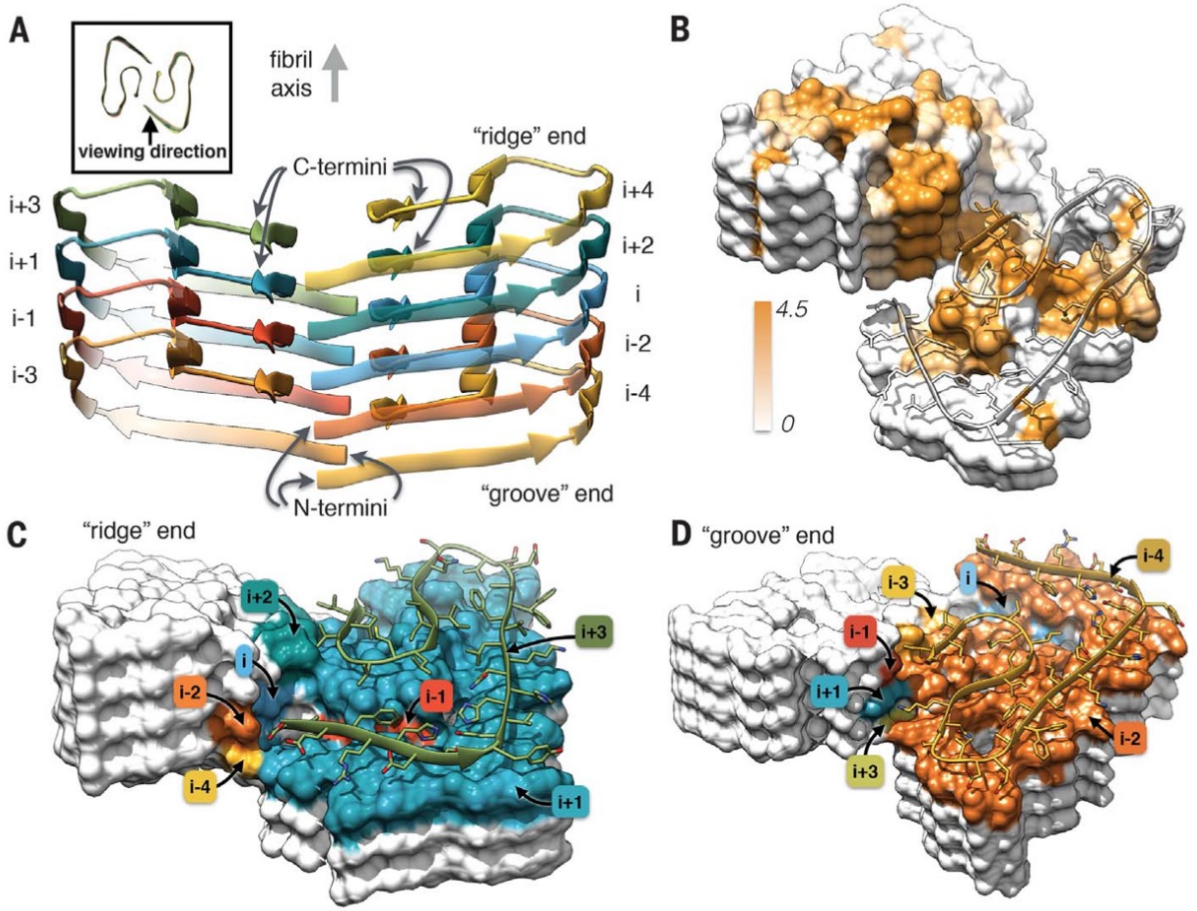

Fig. 4. Details of the Aβ(1–42) fibril architecture. (**A**) Side view of the atomic model showing the staggered arrangement of the nonplanar subunits. (**B**) Surface representation of a fragment of the atomic fibril model. Surface is colored according to hydrophobicity (Kyte-Doolittle scale) [gradient from brown (hydrophobic, 4.5) to white (neutral, 0.0)]. (**C** and **D**) View of the "ridge" (C) and "groove" (D) fibril ends. Only the contact surfaces of the subunits with the respective capping monomer [*i*+3 in (C) and *i*-4 in (D), shown as ribbons] are colored [color coding according to layer number; see (A)].

Three distinct binding sites

Compound	FLINT1 K_{d1}	FLINT2 K_{d2}	Ratio K_d1/K_d2
	nM		
Thio T	**30,350**	**750**	40.5
[^{3}H]Me-BTA-1	ND	ND	ND
BTA-1	**5230**	ND	ND
IMPY-H^b	**43,410**^{b}	**1420**	30.6
IMPY-Me	**35,560**	**1000**	35.6
TZDM	**430**	**120**	3.6
TZPI	**870**	**170**	5.1
BF1	**300**	**120**	2.5

K_{d1} : プローブ濃度を固定し、Aβモノマー濃度を変動させた時の結合定数
K_{d2} : Aβモノマー濃度を固定し、プローブ濃度を変動させた時の結合定数
K_{d1} /K_{d2} : モノマーいくつ分に対してそのプローブの結合部位があるかを示す値

ThT, IMPY-H^b, IMPY-Me→ 30~40モノマーあたり一つの結合部位 (**BS1**)
TZDM, TZPI, BF1→ 3~5モノマーあたり一つの結合部位 (**BS2**)
→２つの結合部位があることの示唆する
　前者(**BS1**)より後者(**BS2**)の方がより多くAβ上に存在するということがわかる

その他、300モノマーあたりに一つ存在するBSもあるという結果が→**BS3**とした

Lockhart A. *et al. J. Biol. Chem.*, **2005**, *280*(9), 7677-84.

FRET (Fluorescence Resonance Energy Transfer)

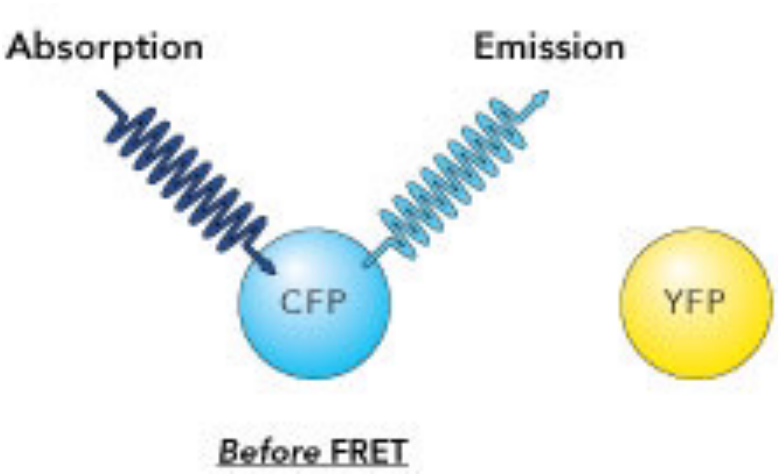

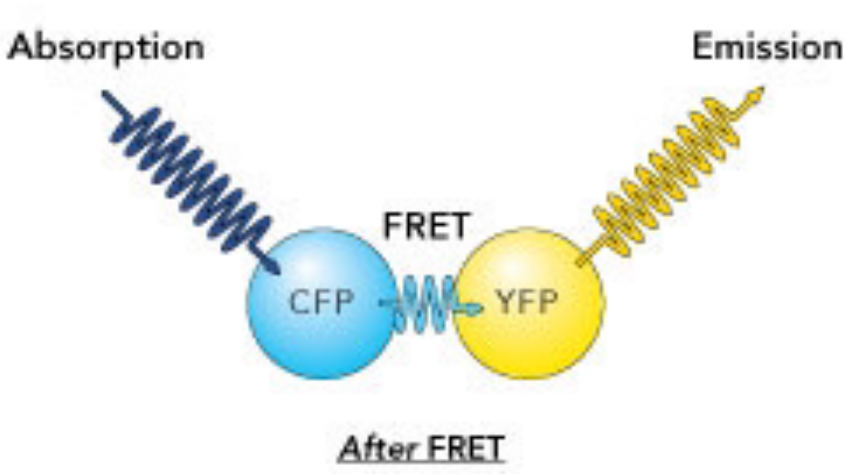

Distance-dependent interaction

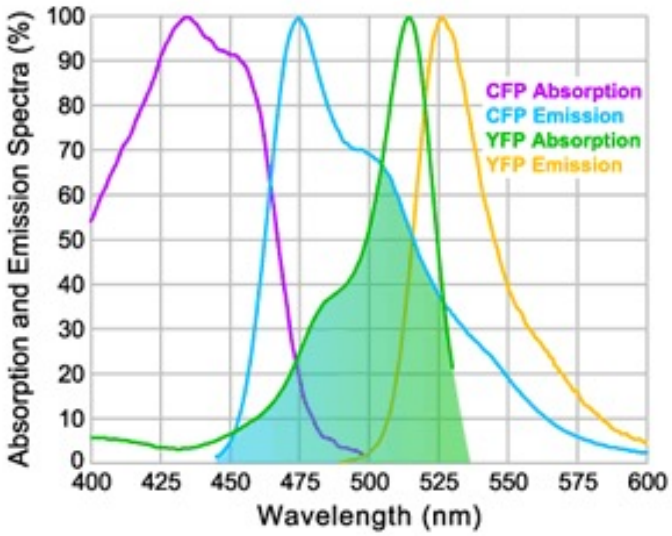

This figure shows CFP (donor) and YFP (acceptor) absorption and emission spectra. Overlap between CFP emission and YFP absorption (shaded region) leads to efficient FRET interaction.

https://www.semrock.com/fret.aspx

Works of Dr. Koide and Dr. Makabe

- **PSAM as a model of *β*-sheet structure**

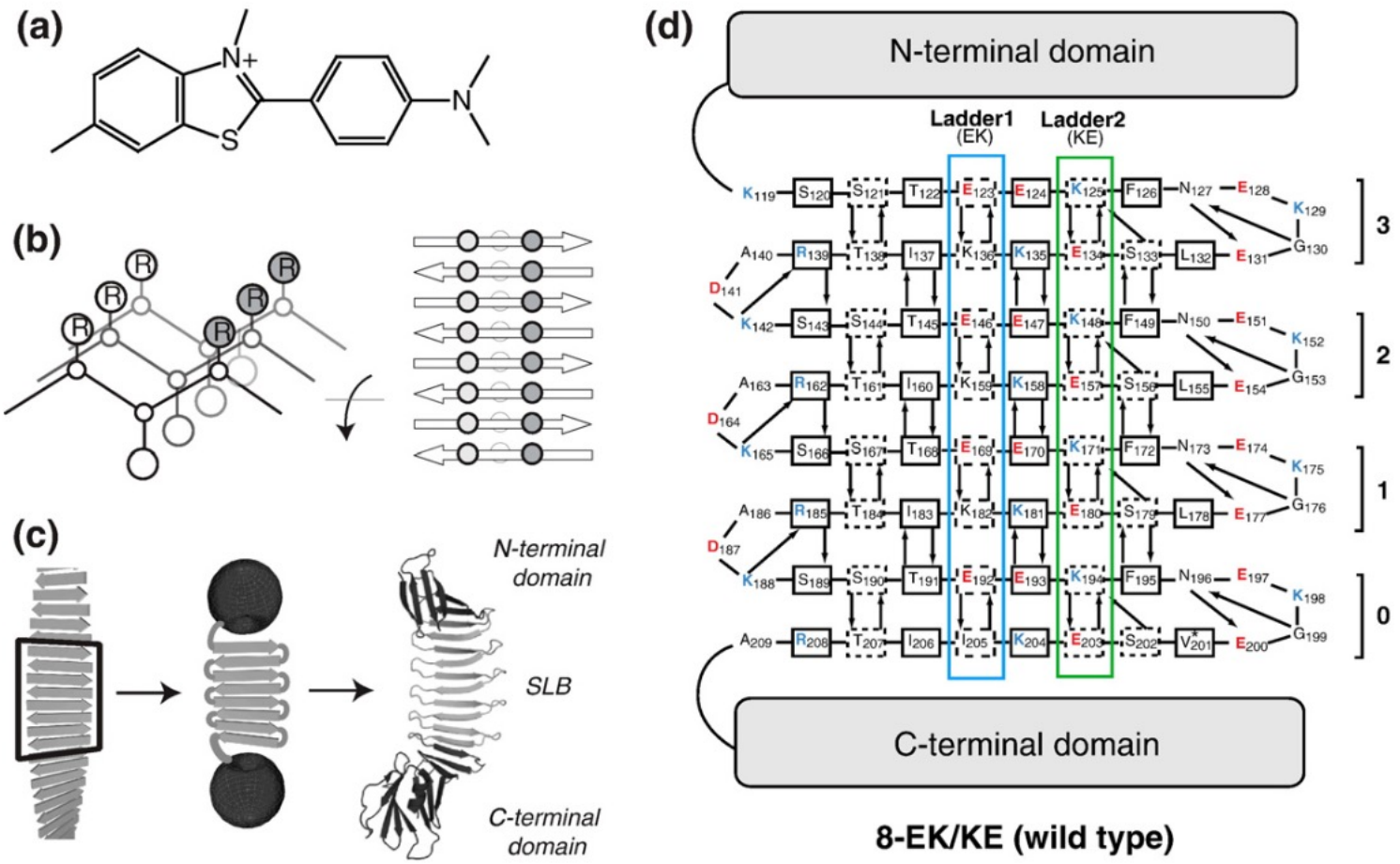

Matthew Biancalana, Koki Makabe, Akiko Koide and Shohei Koide, *J. Mol. Biol.* **2009**, *385*, 1052–1063

Works of Dr. Koide and Dr. Makabe

- **Tyrosine is the key to the binding mode of ThT**

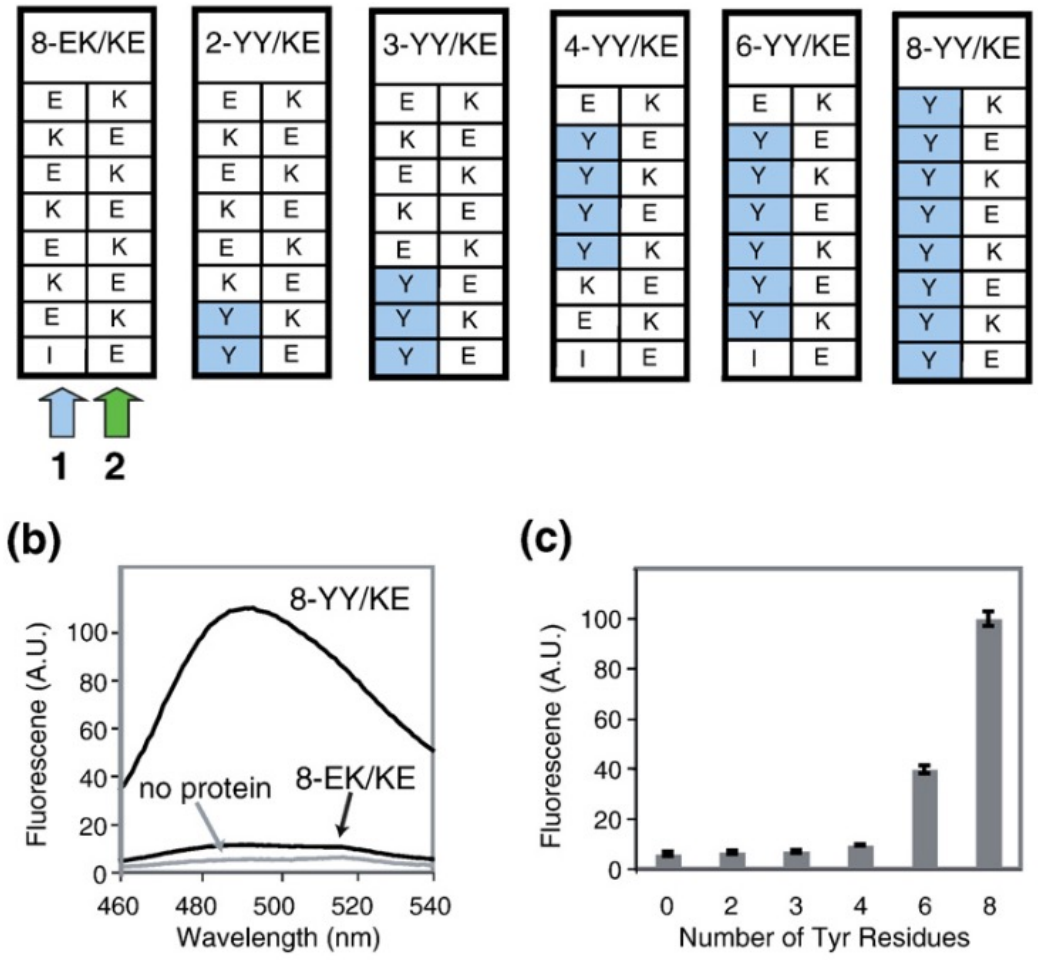

Fig. 2. Design of single cross-strand ladders in the PSAM and their ThT-binding properties. (a) A scheme of single Tyr-ladders of different lengths used in this work. Note that the locations of the Tyr ladder mutations were dictated by our limited ability to specifically introduce mutations at certain positions due to the redundancy of the PSAM gene. (b) Fluorescence emission spectra of 10 μM ThT in the absence and in the presence of 100 μM 8-YY/KE or 100 μM 8-EK/KE. (c) ThT fluorescence emission as a function of the number of contiguous cross-strand Tyr residues. The fluorescence intensity at 485 nm is shown after subtracting the blank (no protein) spectrum of 10 μM ThT, and are normalized relative to the 8-YY/KE signal.

At least 4~6 tyrosines are needed.

Matthew Biancalana, Koki Makabe, Akiko Koide and Shohei Koide, *J. Mol. Biol.* **2009**, *385*, 1052–1063

Works of Dr. Koide and Dr. Makabe

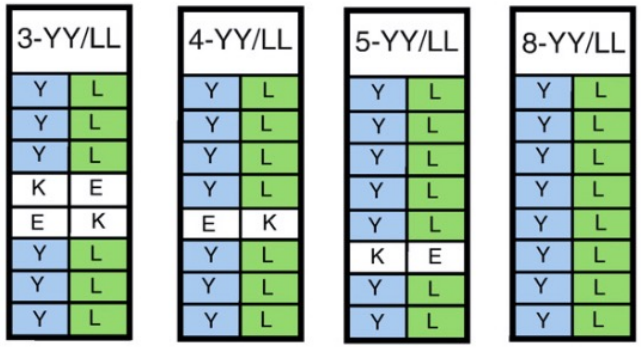

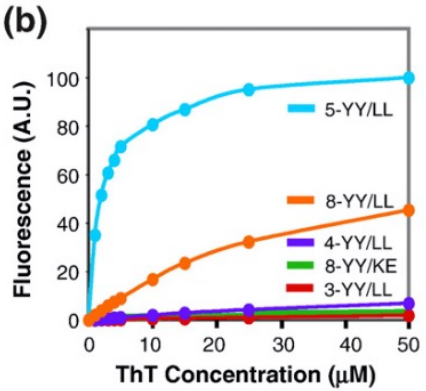

→ **5-YY/LL is the most favorable.**

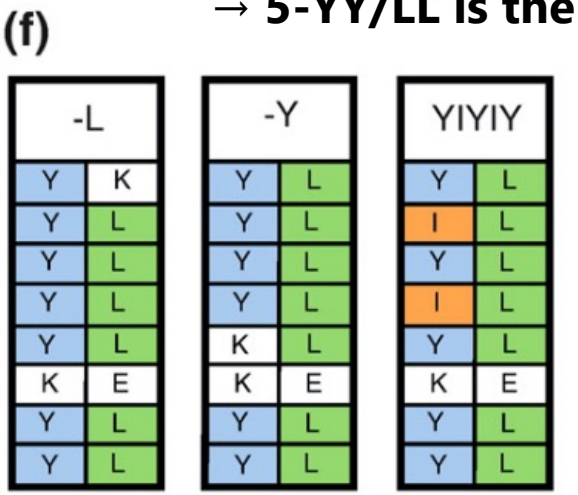

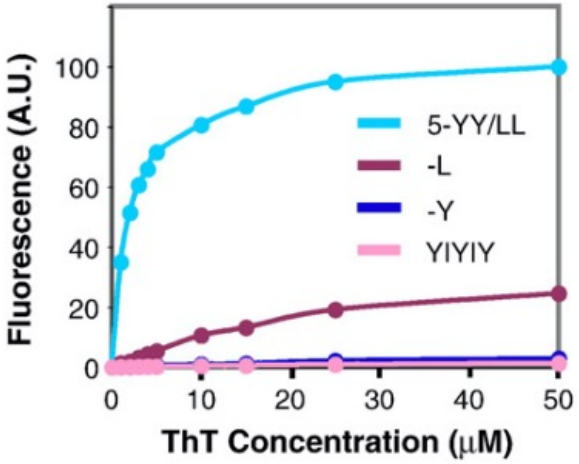

- **Aromatic side chains of** Tyr is important.
- The **Leu ladder** seems to have a secondary role in forming ThT-binding site.

Matthew Biancalana, Koki Makabe, Akiko Koide and Shohei Koide, *J. Mol. Biol.* **2009**, *385*, 1052–1063

Works of Dr. Koide and Dr. Makabe

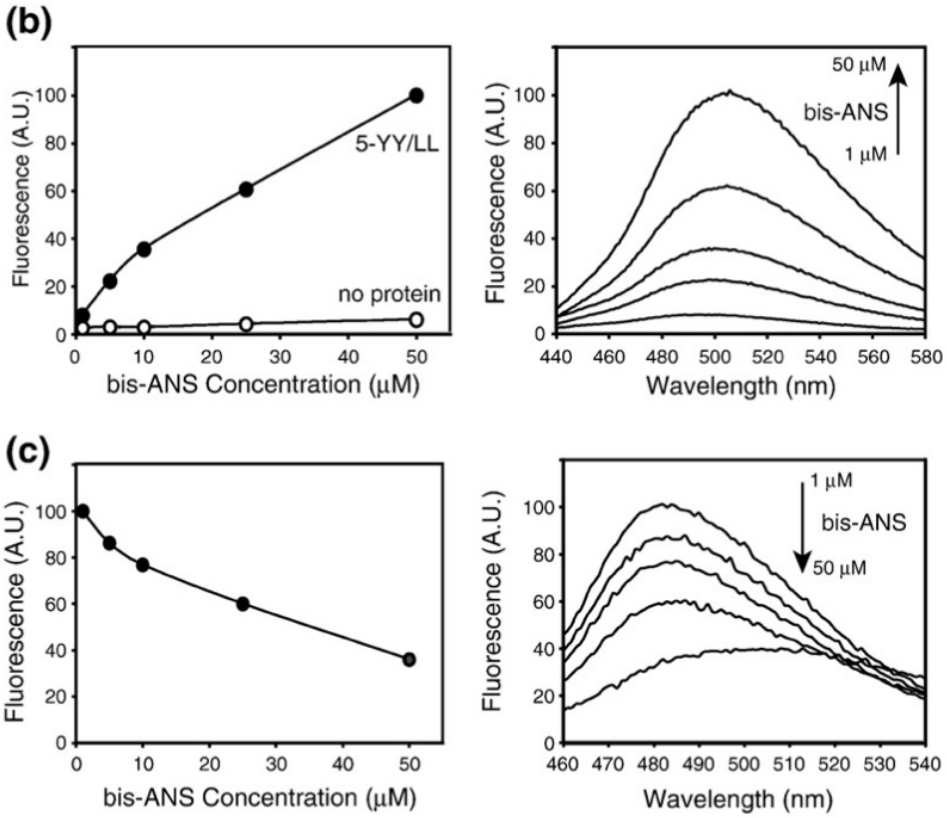

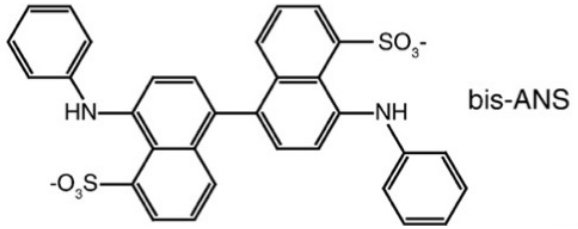

bis-ANS seems to share the binding sites with ThT.

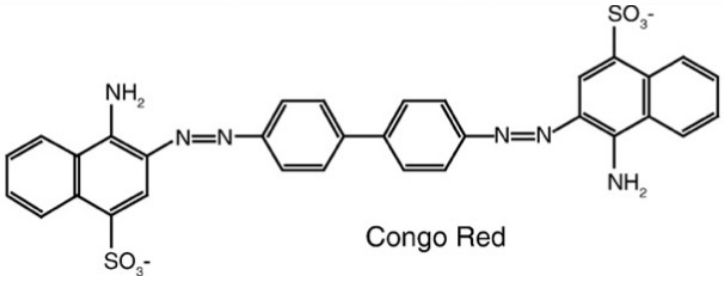

No evidence for binding of Congo Red to 5-YY/LL
→ Binding site of 5-YY/LL is **too small**??
(CR: ~26 Å, ThT: ~15 Å)

Matthew Biancalana, Koki Makabe, Akiko Koide and Shohei Koide, *J. Mol. Biol.* **2009**, *385*, 1052–1063

Co-crystallization with Orange G

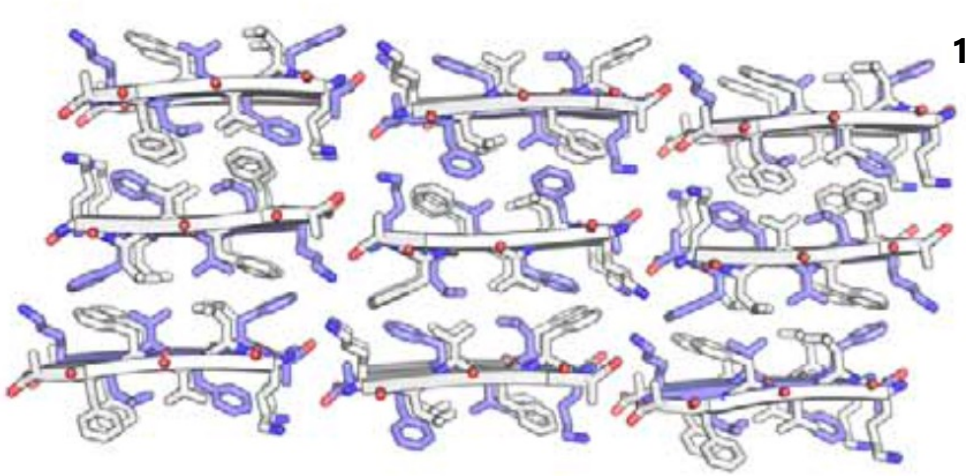

^{16}KLVFFA^{21}

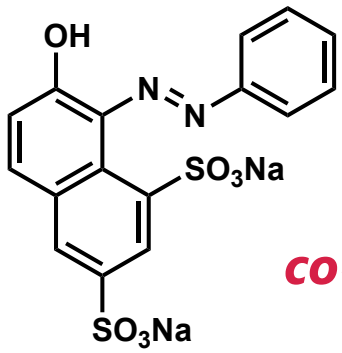

Orange G

co-crystallization

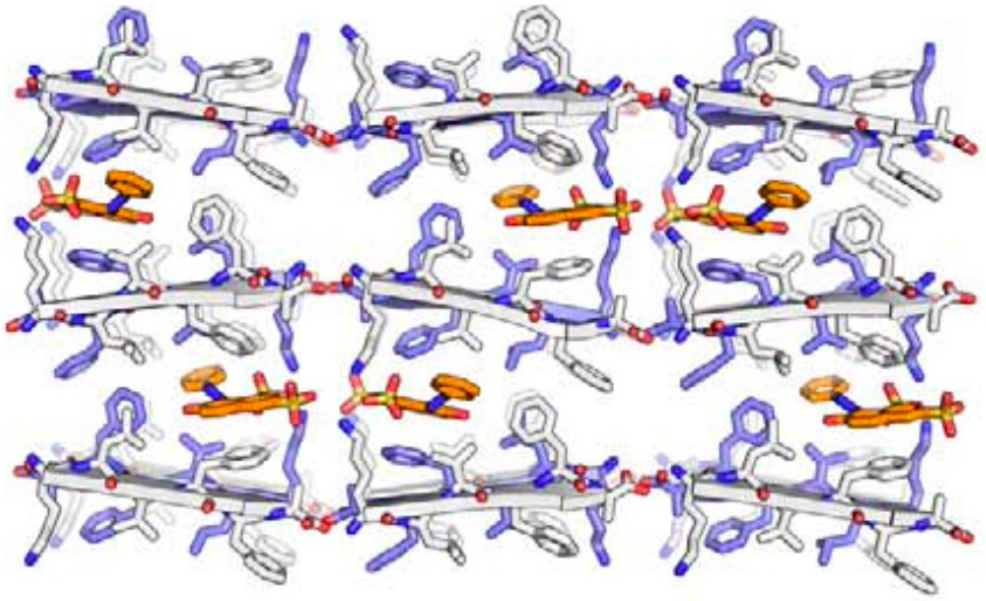

Meytal Landau *et al. PLoS Biol*. **2011**, *9*, 1–13.

Co-crystallization with Orange G

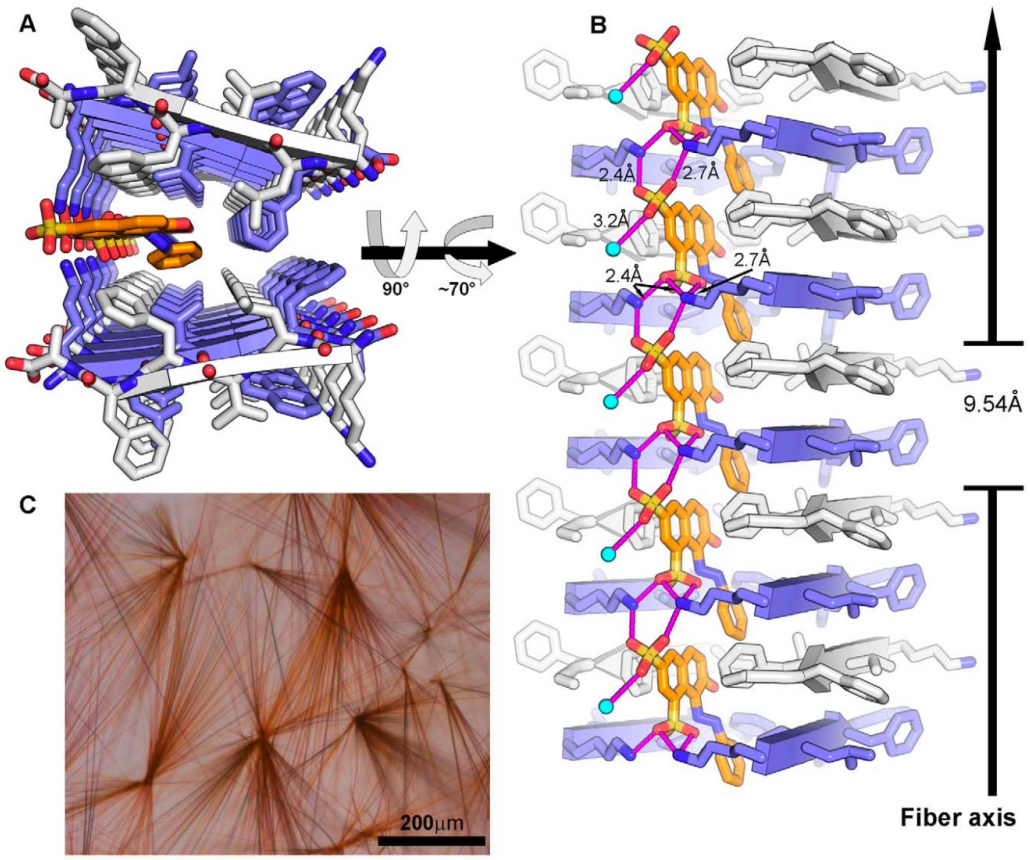

This crystal structure may provide a pharmacophore of A*β*-selective probes??

Meytal Landau *et al. PLoS Biol*. **2011**, *9*, 1–13.

A working model of Aβ oligomers

- **peptide 1a: as a mimic of $A\beta_{17\text{-}36}$**

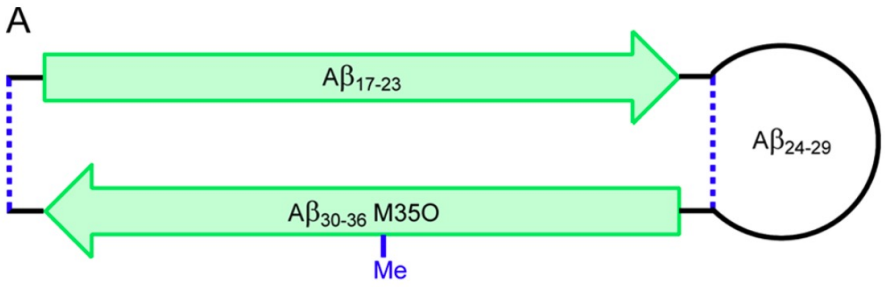

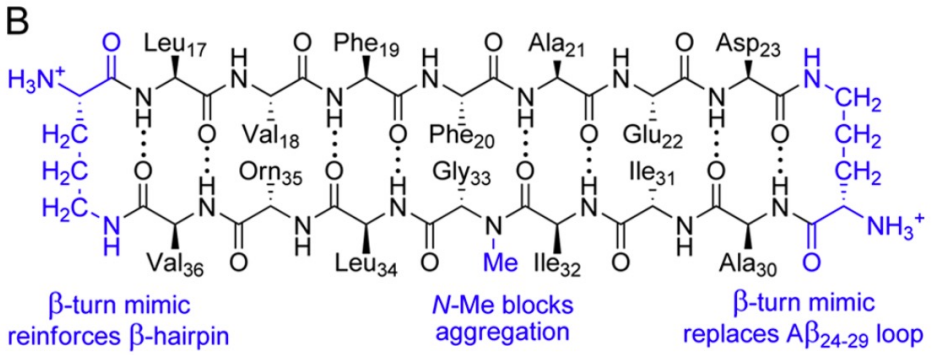

peptide **1a**

The structure of trimers or higher-order oligomers were **not known**.

↓

- ✓ Crystallization was achieved by **modifying side chains** of $A\beta_{17\text{-}36}$.
- ✓ The crystal structure of Aβ trimer provides a **working model**.

Ryan K. Spencer, Hao Li, and James S. Nowick, *J. Am. Chem. Soc.* **2014**, 136, 5595−5598.

Tau selectivity

Structure	Core M. W.	Core length (Å)	Compound name
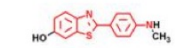	216.2	10.9	PIB
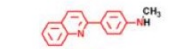	208.2	11.1	BF-158
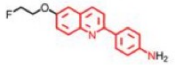	217.3	11.1	THK523
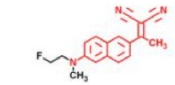	201.2	11.7	FDDNP
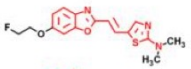	234.2	12.1	BF-227
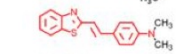	240.2	13.2	DMSB
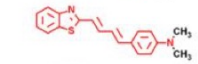	264.2	15.6	PBB1
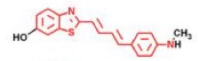	264.2	16.0	PBB2
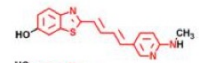	266.3	15.6	PBB3
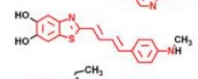	264.2	15.6	PBB4
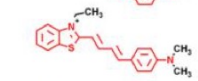	264.2	15.5	PBB5
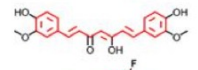	239.3	15.6	Curcumin
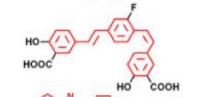	264.2	16.6	FSB
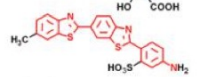	346.4	17.3	Thioflavin-S
	280.2	18.5	BF-189
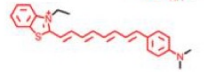	356.5	20.5	DM-POTEB

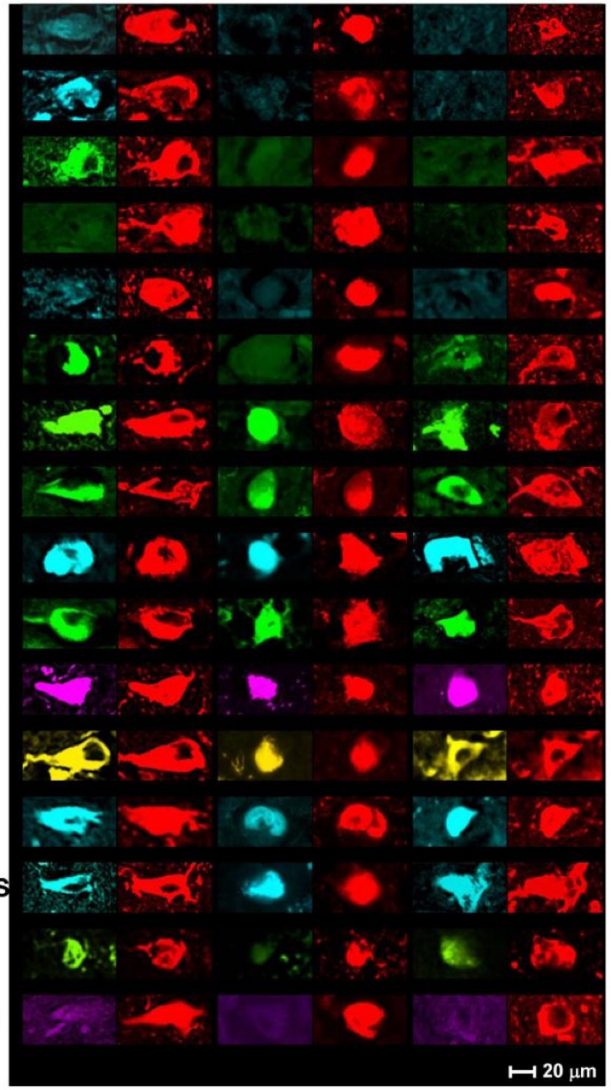

13-19 Å between D & A

↓

Well detected!

***AT8: Anti PHF-tau antibody**

Maruyama M. *et al. Neuron,* **2013**, 79, 1094–1108.

TICT of Tau 1 and Tau 2

Tau 1

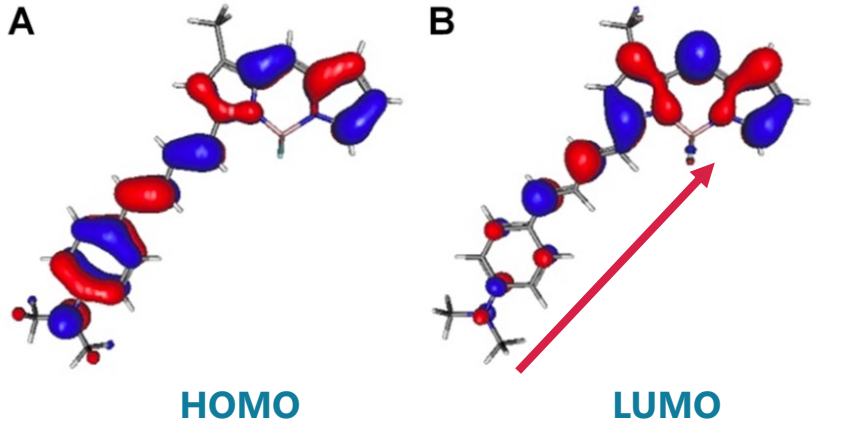

Tau 2

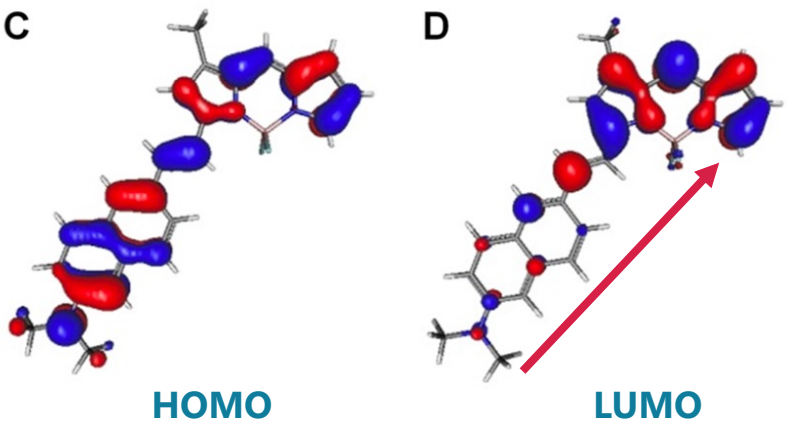

Electron redistribution from the **aniline / aminonaphthalene** in the HOMO to the **BODIPY core** in the LUMO

↓

Involvement of **TICT process** (**large Stokes shift**)

(Large stokes shift contributes to better signal over noise ratio)

Peter Verwilst *et al. J. Am. Chem. Soc.* **2017**, 139, 13393−13403.

Molecular docking studies (Tau 2)

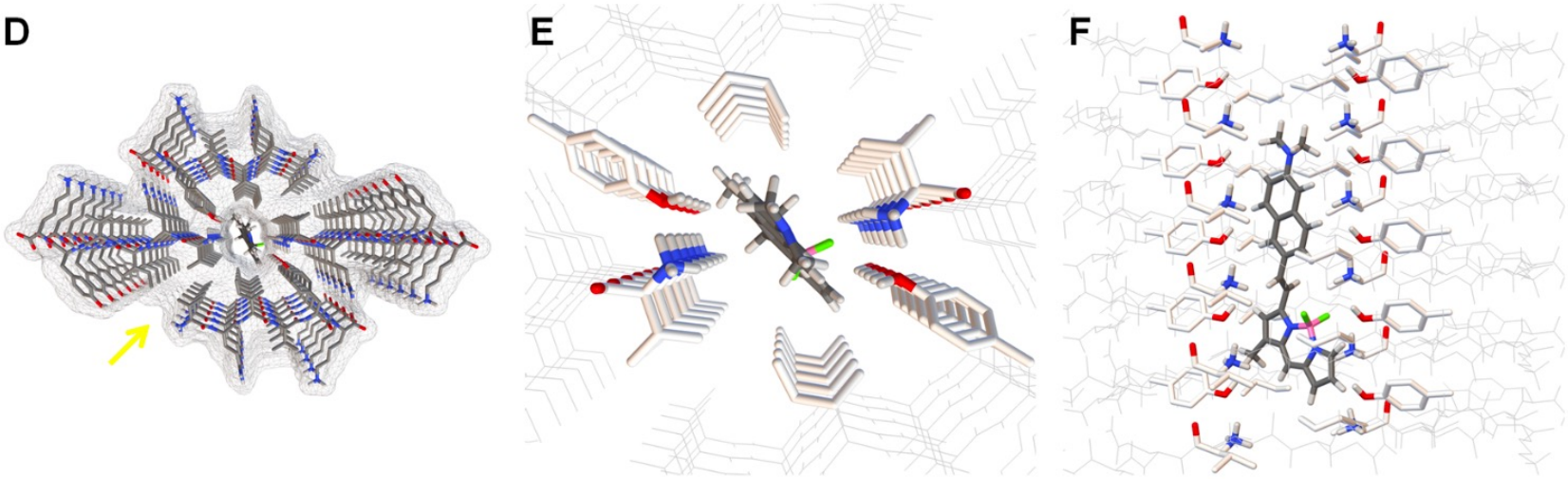

Tau 2 also demonstrated a tight fit in the tunnel.

Peter Verwilst *et al. J. Am. Chem. Soc.* **2017**, 139, 13393−13403.

Check the selectivity of ThT & BAP-1

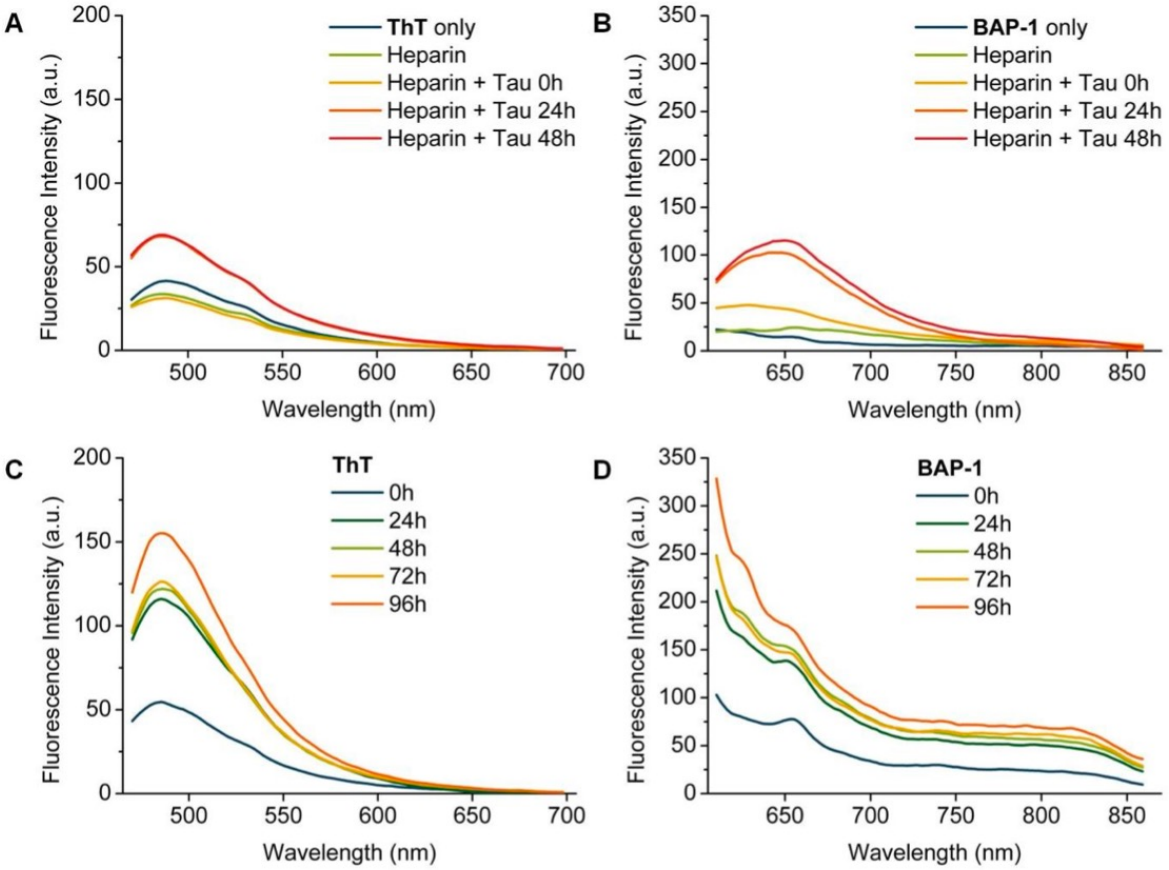

Figure S32. Time dependent fluorescence enhancement of **ThT** and **BAP-1** (10 μM) in the presence of protein aggregates. (A) Emission spectra of **ThT** in the presence of tau protein (10 μM) and heparin (2.5 μM), excited at 450 nm, (B) Emission spectra of **BAP-1** in the presence of tau protein (10 μM) and heparin (2.5 μM), excited at 590 nm, (C-D) Emission spectra of **ThT** and **BAP-1** in the presence of Aβ fibrils (50 μM).

Another example of tau-selective probe

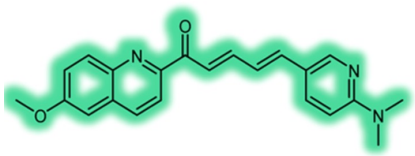

Q-tau 4

- ✓ Tau λ_{em} = 630 nm
- ✓ Tau K_d = 16.6 nM

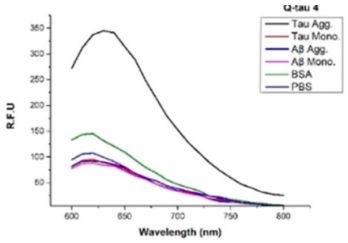

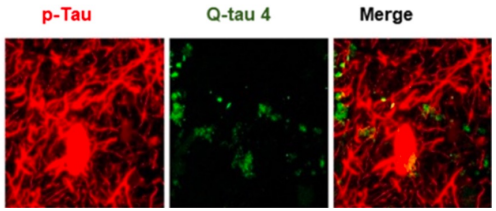

C

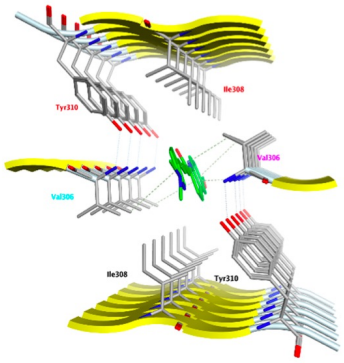

D

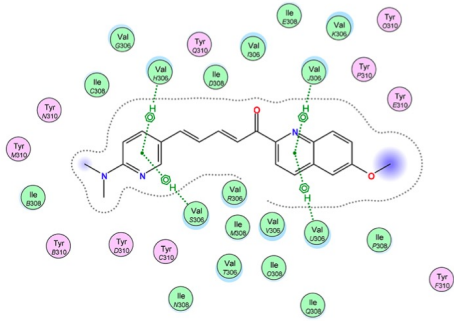

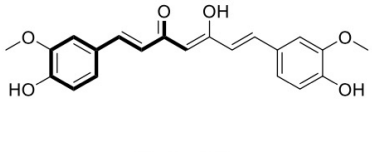

Curcumin

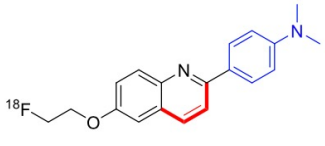

^{18}F-THK-5377

tau K_i = 51 nM

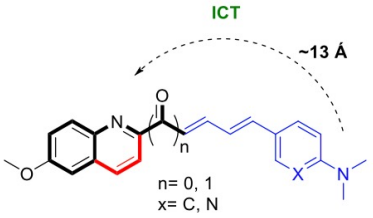

Q-tau

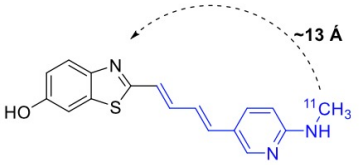

^{11}C-PBB3

50-fold tau selective over Aβ

The design of this probe also follows **two hypotheses of tau-selectivity**. Molecular docking study demonstrated the **high affinity** to ^{306}VQIVYK^{311} tunnel as well.

Ahmed A. Elbatrawy *et al. ACS Sens*. **2021**, *6*, 2281-2289.